ANALYSES OF THE ANNEALING PROCESSES AND THE EFFECTS OF PLASMA TREATED SUBSTRATE SURFACES FOR MOS DEVICES

BY

DANIEL Y. CHUNG

A Thesis
Submitted to the Faculty of Graduate Studies
in Partial Fulfillment of the requirments
for the Degree of

MASTER OF SCIENCE

Department of Electrical Engineering
University of Manitoba
Winnipeg, Manitoba

ISBN 0-315-81752-6

ANALYSES OF THE ANNEALING PROCESSES AND THE EFFECTS OF PLASMA TREATED SUBSTRATE SURFACES FOR MOS DEVICES

BY

DANIEL Y. CHUNG

A Thesis submitted to the Faculty of Graduate Studies of the University of Manitoba in partial fulfillment of the requirements for the degree of

MASTER OF SCIENCE

To Anthony,

Clare,

and Mei

ABSTRACT

The annealing processes and the effects of plasma treatments of the silicon substrate surface on the performance of MOS devices have been systematically investigated. The silicon dioxide (SiO_2) films used for the MOS devices were fabricated by an ECR Microwave PECVD process at the temperature of 300°C. The high frequency and the quasi-static frequency capacitance-voltage methods were adopted to characterize the midgap interface trap density and the oxide fixed charge density. The results show that apart from the atomic hydrogen, the molecular hydrogen plays as well an important role in the annealing processes for the reduction of the interface traps, and that SiO defects also act as interface traps besides silicon dangling bonds. A new multi-reaction model that includes the molecular hydrogen and the SiO defects is presented. This model explains well the annealing processes under various annealing ambients. We have also studied the effects of substrate surface treatment by a plasma produced in various gases. Nitrogen plasma treatment reduces the interface trap density from $10^{12}cm^{-2}eV^{-1}$ to $10^{11}cm^{-2}eV^{-1}$ after PMA. The silicon substrate surface treated with oxygen plasma may yield an interface trap density in the order of $10^{10}cm^{-2}eV^{-1}$, which makes the ECR microwave PECVD films comparable to the high quality thermal oxide.

ACKNOWLEDGMENTS

I would like to thank my advisor, Professor Kwan C. Kao, for his assistance, encouragement and patience throughout the development of this thesis.

I also would like to thank the helpful individuals of the Materials and Devices Research Laboratory, especially K. Westra and M. Jin.

Appreciations are also given to C. Shafai for taking AFM images for the oxide films.

Sincere thanks are also given to Dr. D. Liu, K. Lin, A. Chan and T. T. Chau for their valuable discussions.

Special thanks are given to Mei for her understanding and support throughout the period in the preparation of this thesis.

TABLE OF CONTENTS

LIST OF FIGURES

LIST OF TABLES

CHAPTER 1

INTRODUCTION.

The advancement in VLSI technology has grown very rapidly in recent years. Microprocessors consisting of more than 2.5 millions transistors per chip with a gate length of 1.2 micron have been in production for more than two years. Memory chips consisting transistors with submicron gate length will be in production in the near future. There is no doubt that the dimensions of the transistors will continue to shrink to provide a higher density of devices per unit area and to reduce the response time of the transistors.

All components of a transistor have to be reduced in size in order to maintain its normal performance, for example, an acceptable turn-on threshold voltage. An enormous amount of work is being done toward this goal. A significant portion of this research is to scale down the thickness of the gate oxide. Traditional thermal oxidation method can produce silicon dioxide films with a thickness as low as 70Å, but they have to be grown at a temperature over 900 °C and have a very low yield. At such high temperatures, the diffusivities of the impurity dopants inside the silicon which are exponentially proportional to the temperature become very high and hence the distribution profile of the dopants undergo a significant change in each oxidation step during the fabrication process. As the complexity of the integrated circuit increases, the number of oxidation steps as well as the number of processing steps will increase. It makes the fabrication process very hard to control in terms of the distribution profile of various dopants on which the characteristics of the device depend. Rapid thermal oxidation may reduce the processing time and may thus

minimize the diffusion related problem [1]. However, another drawback of this process is the high temperatures involved, which will cause stress in the wafer and thus create defects.

To avoid or to minimize such diffusion related or temperature sensitive phenomena involved in high temperature processing, plasma enhanced chemical vapor deposition (PECVD) process for low temperatures (<300 °C) deposition of silicon dioxide films has been developed. Several techniques based on this process have been reported recently. Each technique has its own advantages and disadvantages. The radio frequency (rf) PECVD can produce films with a high deposition rate, but the films suffer from the radiation and ion bombardment damages [2]. These damages could be reduced by using a remote rf PECVD technique [3]. The microwave electron cyclotron resonance (ECR) PECVD [4] can also produce films but it requires a high carrier gas flow and a low operating pressure in the order of mTorr, which results in a much lower deposition rate and the deposited films would suffer from vacuum UV radiation damage. This kind of damage can be reduced to an acceptable level by using a downstream ECR PECVD technique [5]. Recently the Materials and Devices Research group at the University of Manitoba has developed a species selector and energy controller (SSEC) [6] to separates the plasma source from the deposition chamber. Using some of the techniques described above, several groups have successfully produced SiO_2 films of the order 100Å at relatively low temperature (300 - 450°C) with electrical properties approaching those of high quality thermal oxides grown at temperatures higher than 1000 °C. The major advantages of the PECVD techniques are that the SiO_2 films can be produced at much lower temperatures and the films are stoichiometic and uniform in composition, and their properties are independent of thickness [7].

The basic difference between the PECVD and the thermal oxides is that the thermally grown oxide is formed by the diffusion of oxygen species to the Si-SiO_2 interface while the PECVD oxide is formed layer by layer on the original silicon surface. It can be imagined that the surface condition of the silicon substrate surface is more vital in the case of the PECVD oxide films because the original silicon surface which latter becomes the Si-SiO_2 interface is likely to contain more contaminants from the environment. Also the abrupt interface between the PECVD films and the silicon substrate is believed to have a higher density of dangling bonds due to the incompatibility between the silicon substrate lattice and the silicon oxide lattice. Both of these creates charges and defects at the Si-SiO_2 interface thus resulting in a higher interface trap density, and hence affecting the threshold voltage and the surface carrier mobility of the MOS device. This, in turn, degrades the general performance and the response time of the device. The degradation becomes more significant as the device dimension is scaled down because the role played by the interface becomes more important as the oxide thickness is reduced to the 100Å region because the channel is not as deep as larger devices. Therefore the feasibility of the PECVD oxide to be used as the gate oxide still depends greatly on the degree of contamination on the surface of the silicon substrate. Conventional wet cleaning is good enough for thermally grown gate oxides of thicknesses down to 200Å but not for PECVD oxides because the substrate surface is highly exposed to contaminants such as hydrocarbons and other organic compounds in the cleaning fluid or in the air. Therefore, *in-situ* dry cleaning is a good alternative to the conventional wet cleaning method. Dry cleaning is usually performed in vacuum and the chance of contaminating the surface is significantly reduced. Several groups have reported the effectiveness of dry cleaning by

using microwave ECR plasmas, such as O_2 plasma [8] and H_2 plasma [3,9] in terms of the removal of the native oxide and the surface contaminants.

Another way to reduce charge defects is by thermal annealing. The annealing process involves the annealing of the device at 400°C in a forming gas (10% H_2 in N_2) for polysilicon gate devices, or in a pure N_2 environment for devices which have active metal elements such as aluminum and copper as electrodes [10]. The function of annealing is to reduce the contact resistance for the source and drain in the MOS system and to reduce the interface trap density by passivating the dangling bonds by hydrogen. For thermally grown oxide films, such an annealing process is able to reduce the interface traps density from 10^{12} cm^{-2} eV^{-1} down to the order of 10^{10} cm^{-2} eV^{-1}. None of today VLSI circuits would function properly without going through such an annealing process to reduce the interface traps to an acceptable level. This process is even more important for PECVD oxide films because the interface trap density is in the order of 10^{14} cm^{-2} eV^{-1} as deposited without annealing. It has been reported [11] that the interface trap density of the PECVD SiO_2 films can be reduced through a proper annealing process to a level of about 10^{11} cm^{-2} eV^{-1}. Although the annealing process has been widely used in all integrated circuit industries, the actual mechanism of the annealing process is not fully understood. The generally accepted model for the annealing mechanism is the two reaction model proposed by Reed and Plummer [12]. This model fits comparatively well with the experimental data for post metallization annealing (PMA). One major drawback is that it cannot explain why there is a decrease of the interface trap density when bare oxides without electrodes are annealed in an atomic hydrogen free medium. It is likely that the two reaction model is too simplistic for describing the interface trap annealing process. However it is a good starting point for the development of more complete models.

In this thesis, Chapter 2 give a detailed description of the physical structure and the chemical composition of the Si-SiO_2 interface as well as a few models describing the behavior of the interface. Chapter 3 presents a numerical analysis of the annealing mechanism and proposes a more complete annealing model. Chapter 4 describes the effects on the interface trap density and the fixed charge density of various plasma treatments of the silicon substrates prior to the deposition of SiO_2 films. Finally, the conclusions are given in Chapter 5. All the details about the sample preparations, the C-V measurement method and the computer program for the calculation of the interface trap densities are given in the appendice.

CHAPTER 2

PHYSICAL STRUCTURE, CHEMISTICAL COMPOSITION AND DEFECTS OF THE Si-SiO_2 INTERFACE

The performance of the MOS field effect transistors depends strongly on the quality of the gate oxides. A high quality oxide film should contain only minimal and acceptable amount of defective charges at the silicon substrate-oxide (Si-SiO_2) interface and in the oxide bulk. The acceptable interface defect density by the industries is below 10^{-11} $eV^{-1}cm^{-2}$. The concentrations of these defects depend entirely on the fabrication process which includes the pre-oxidation or the pre-deposition substrate cleaning process, as well as the oxidation or the deposition parameters such as temperature, gas pressure, etc. The amount of these defects can be minimized by choosing an appropriate oxidation or deposition conditions. They can also be be further reduced by annealing the devices in a suitable environment. However, to produce high quality gate oxides, it is important to have a clear picture about the origins and the nature of the interface defects.

Extensive efforts have been made in the past to study the mechanisms responsible for the generation of the defective charges present in the Si-SiO_2 interface and the oxide bulk, and the methods of minimizing them [10,13,14,15]. There are four kinds of defective charges, namely, the interface trap charges, the oxide fixed charges, the oxide trapped charges and the mobile ion charges. Amount these charges, the interface trapped charges and the interface fixed charges are very similar in nature and locate very close to each other.

2.1 Physical Structure of the Si-SiO_2 interface

Silicon dioxide has been used as an insulator in MOS transistors for some thirty to forty years. Many scientist and engineers [16,17] have attempted to understand the structure of the oxide layer and the structure of the Si-SiO_2 interface. In doing so, some of the questions regarding the micro mechanisms of oxidation and of the interface traps should be answered.

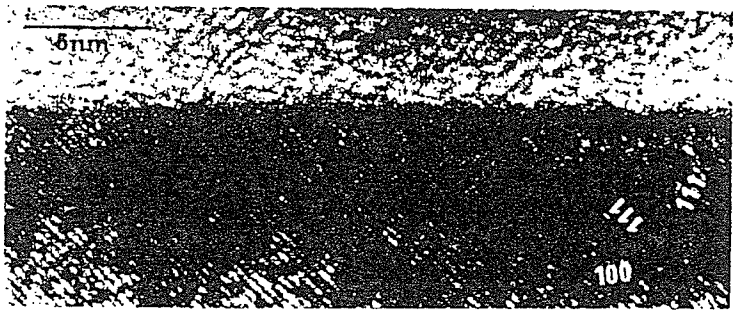

Figure 2.1: Cross sectional TEM image of the Si-SiO_2 interface (thermally grown SiO_2)

Using a cross sectional transmission electron microscope (TEM), Krivanek et al [18] have reported the images of the Si-SiO_2 interface in 1978. The image is shown in Figure 2.1, in which the resolution for silicon crystal was 3Å and that for SiO_2 was not known. However, this image shows clearly a transition from the silicon crystal to amorphous silicon oxide. There is a sharp transition. Because of the resolution limit, it was not possible to determine the structure of the interface. We still do not know whether it is a crystalline silicon to amorphous silicon oxide abrupt interface or it has an interfacial layer present in between. If there is an interfacial layer, then this layer could be amorphous silicon, crystalline silicon oxide of some particular forms or a mixture of amorphous silicon with amorphous silicon oxide. It is generally believed that the interfacial layer consists of

cristobalites, a common form of crystalline SiO_2 formed simply by inserting oxygen atoms between silicon atoms [19]. With a lattice parameter of 40% larger than that of the silicon crystal, the formation of cristobalite on top of the silicon substrate will create a considerable amount of stress and thus make the structure unstable and unrealistic. Another thought of the interface is that the interface is abrupt with no transition layer in between. But this seems to be violating the basic thermodynamic theory because an abrupt transition implies that the entropy contained inside the system would be infinite. It has also been suggested that the interface layer is a mixture of amorphous silicon and amorphous silicon oxide. The amorphous silicon is present because the lattice structure is upset by the invading oxygen atoms.

Recently, using a high resolution transmission electron microscope (HRTEM), Ourmazd and Bevk [20] have reported that there is indeed a crystalline structure at the Si-SiO_2 interface. Their results about the '110' and the '$1\bar{1}0$' lattice images are shown in Figure 2.2. The structure of a unit cell of silicon crystal is shown in Figure 2.3(a) and the lattice planes are described schematically in Figure 2.3(b). The notations of '110' and '$1\bar{1}0$' represent particular surfaces of the unit cell.

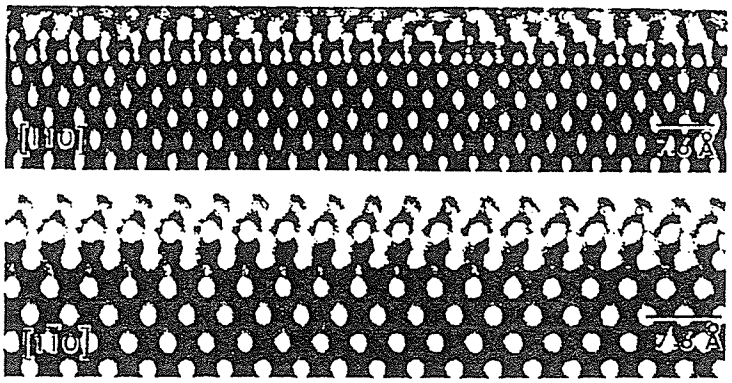

Figure 2.2: HRTEM images of the Si-SiO_2 interface (thermally grown SiO_2)

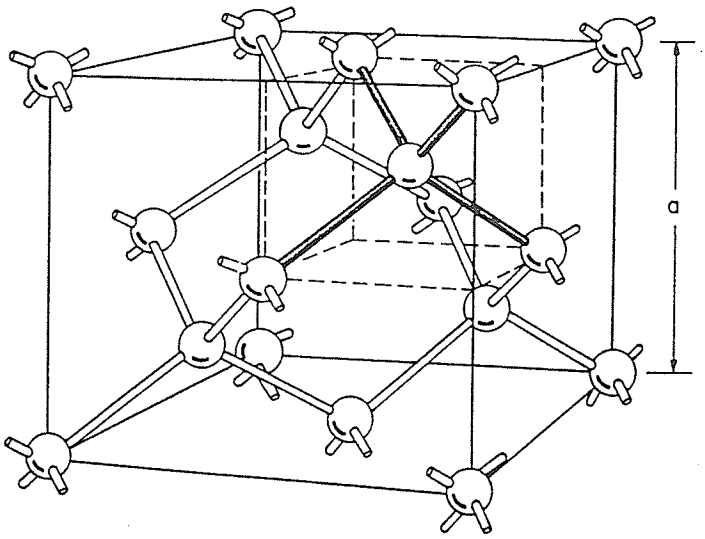

(a)

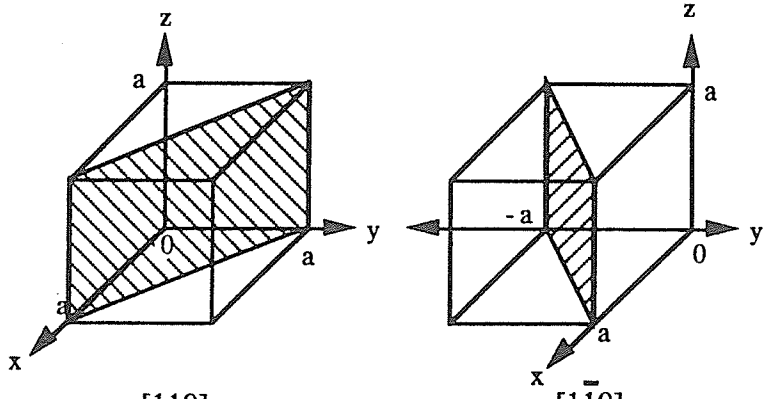

(b)

Figure 2.3: (a) Atomic structure of silicon crystal (b) [110] and [1$\bar{1}$0] planes

It can be seen clearly that there is a distinct crystalline layer of thickness of about 7Å at the Si-SiO_2 interface. The interface layer looks totally different from the two different direction suggesting that the structure of this layer has a two fold symmetry. Since the oxide displays a very complicated image and the pattern of the image probably has a very complicated correlation with the positions of the silicon atoms and the oxygen atoms, there is no direct method to determine the structure of the oxide. Computer simulation has been used to match the HRTEM images. This is known as the Si-SiO_2 bulk structure called the tridymite shown in Figure 2.4. Five monolayers are found within the 7Å transition layer but it is important to note that the tridymite might not be the unique structure that fits the experiment images. It could also be another unknown form of oxide.

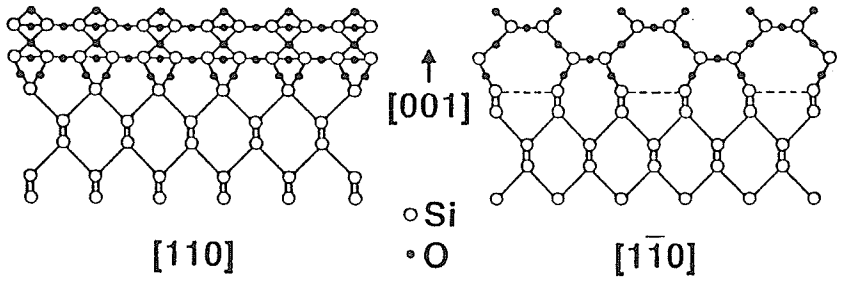

Figure 2.4: Two dimensional representation of the structure of tridymite

2.2 Chemical Composition of the Si-SiO_2 interface

Although the HRTEM images provide a better understanding about the general structure of the Si-SiO_2 interfacial layer, it still could not explain the physical and chemical nature of the interface defective charges. A controversial issue about whether the Si-SiO_2 interface consists of any composition other than SiO_2 still has not been resolved. Due to the

mismatch between the lattice structure of silicon crystal and the lattice structure of the tridymite, stress exists at the interfacial layer which might cause defects. Such defects could be in the form of SiO structures. In the silicon oxygen system, the only equilibrium phases that can coexist are Si and SiO_2. If any SiO phase exists, a large force is required to stabilize the system. However, the existence of the SiO phase has been proposed by Aspens and Theeten [21] based on the ellipsometry results of different photonic energies fit to a variety of models. The fit is poor for an abrupt, stoichiometric interface or a mechanical mixture of silicon and silica. A mechanical mixture only changes the amplitude of the Si and SiO_2 peaks. But, a chemical mixture of silicon and oxygen atoms gives a good fit and the best one is for Si and $SiO_{0.4}$. This finding is consistent with the numerical analysis given in Chapter 3. Using the well known fact that SiO_2 will decompose in the presence of Si at high temperatures (>900 °C).

$$Si + SiO_2 \rightarrow 2\ SiO \tag{2.1}$$

SiO is volatile at temperatures larger than 750 °C and therefore the SiO_2 will continue to decompose at temperatures higher than 900°C. This decomposition may be one of the origins of electrical defects because the presence of SiO is generally believed to be a form of electrical defects at the Si-SiO_2 interface [22]. The formation of electrical defects and voids are shown schematically in Figure 2.5.

The electrical defects are formed at high temperatures due to the acceleration of the formation of SiO. The content of SiO could be minimized by sufficient supply of O_2 to reoxidize the SiO species. If oxygen is not available, voids are formed due to the large amount of SiO_2 decomposed.

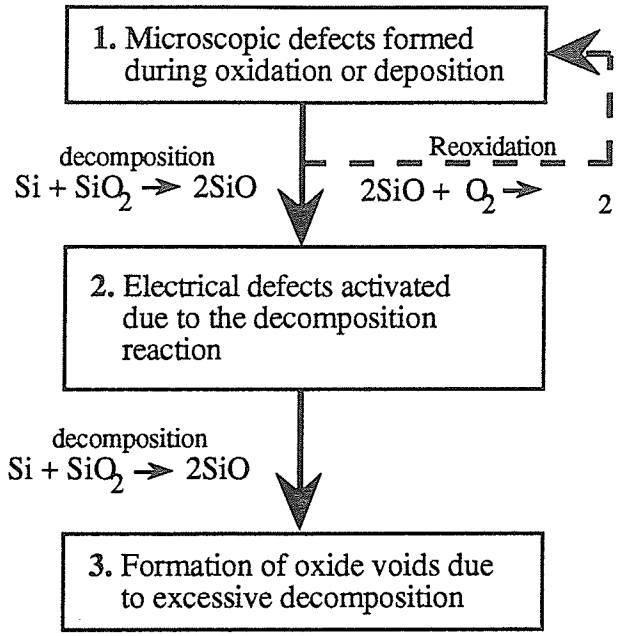

Figure 2.5: Schematic diagram illustrating the formation of electrical defects and oxide voids

2.3 Defective Charges of the MOS System

Electrical measurements are by far the most powerful and widely used methods to probe the defects in the MOS system. Although they are not the direct methods to look at the Si-SiO_2 interface, the information they provide is very useful because the electrical characteristics are one of the major interest to quality determination and control. The Capacitance-Voltage (C-V) method and the Current-Voltage (I-V) method are used for determining all kinds of defective charges in the MOS system. These charges are the interface trap charge, the oxide fixed charge, the oxide trapped charge and the mobile ion charge. The spatial locations of these charges are shown in Figure 2.6.

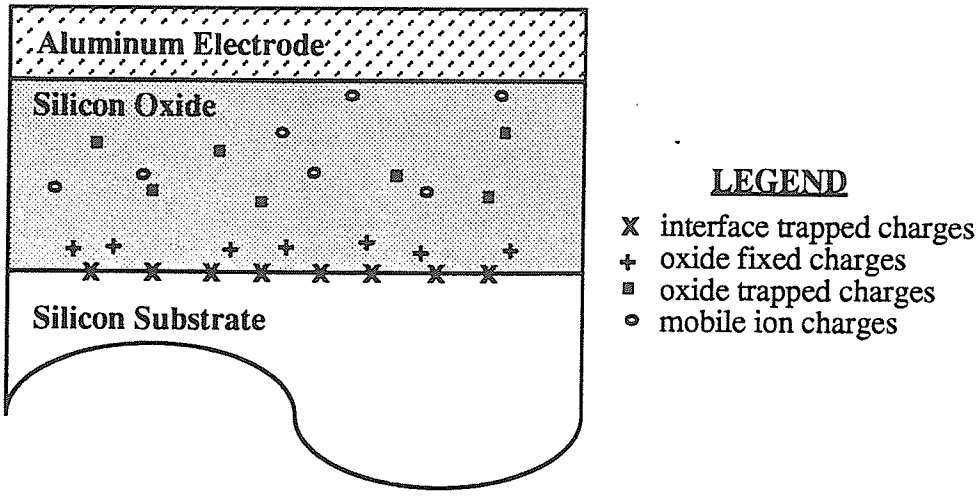

Figure 2.6: Spatial Locations of four kinds of defective charges

2.3.1 Interface Trapped Charge and Oxide Fixed Charge

The interface trapped charge is located within 10Å from the Si-SiO_2 interface. The net charge could be positive or negative because both hole traps and electron traps are presence.Various models have been put forward for the interface traps. These include silicon dangling bonds, misfits, dislocations, excess oxygen atoms and oxygen deficiency [23]. The most widely accepted model is the silicon dangling bond model. The density of the interface traps located at the middle of the silicon band gap, referred to as the midgap density (D_{it}), is generally used to represent the interface trap level for the devices because the accuracy of the measurements of the trap densities drops as the energy level of the traps move toward the band edges.

The difference between the thermally grown oxides and the PECVD oxides could be due to two factors. First, the Si-SiO_2 interface for the PECVD oxides has a much higher chance of getting impurities contamination. Second, the the fabrication process for these two types of oxides are totally different. For thermally grown oxides, the Si-SiO_2

interface structure has been discussed in detail in the previous sections. However, for PECVD oxides, the Si-SiO_2 interface structure is unknown up to today. The surface construction kinetics has yet to be found, possibly by means of more sophisticated techniques such as scanning tunnelling microscopy. It may have an interfacial layer similar to that of thermal oxides but the crystalline structure is expected to consist of more defects such as stacking faults and micropores which tend to lead to a high interface trap density. The interfacial layer might not even have a structure of tridymite. A high temperature annealing (>900°C) after deposition may reduce the trap density because high temperatures enhance the diffusivities of the silicon and oxygen atoms, which, similar to thermal oxidation, help the atoms to rearrange themselves.

The oxide fixed charge (Q_f) is the charge located at about 30Å from the Si-SiO_2 interface. This charge can be regarded as a charge sheet located at the Si-SiO_2 interface which does not change over different surface potential (Ψ_s). Early study has shown that the oxide fixed charge is reproducible [24]. This means that for a certain set of growth parameters, the amount of oxide fixed charge present is unchanged. It is also independent of the impurity concentration in the silicon substrate and the defects in the oxide bulk. The oxide fixed charge is stable under biased temperature ageing condition, indicating that this oxide fixed charge is attached to the interface over a wild range of Ψ_s. Deal et al [14] have suggested that ionic silicon resulting from incomplete oxidation at the interface may be the prime candidate for the oxide fixed charge.

Although the interface trapped charges and the oxide fixed charges appeared differently from the electrical measurements, there is no apparent reason why they are different in nature. The major reason for this is that they are both located so close to the Si-SiO_2 interface and therefore their compositions and structures are very similar. Several

investigators have shown that the oxide fixed charge may be atomically the same. They are different only in terms of their energy level. The interface trapped charges have energy levels within the silicon band gap, thus their occupancy can be changed by the gate bias. However, the energy levels of the oxide fixed charges may be located outside the band gap, this is why their occupancy cannot be changed. The energy diagram for the interface trapped charges and the oxide fixed charged is shown in Figure 2.7.

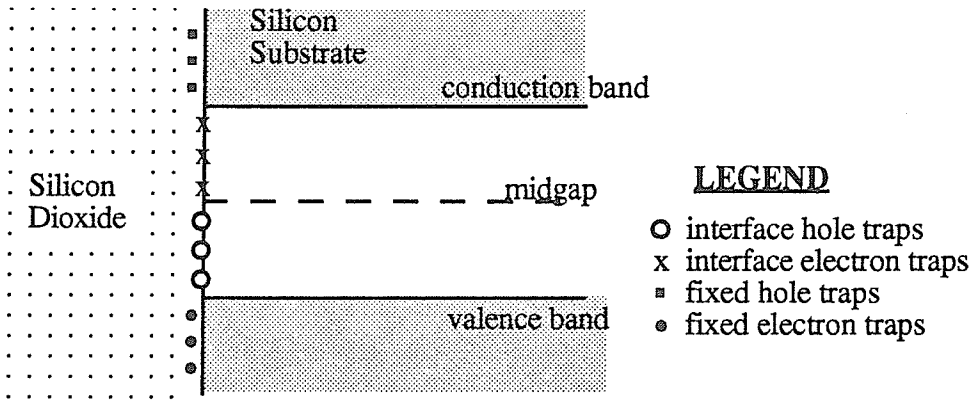

Figure 2.7: Locations of electron and hole traps near the Si-SiO_2 interface

2.3.2 Oxide Trapped Charge and Mobile Ion Charge

The oxide trapped charge can be located anywhere between the Si-SiO_2 interface and the metal-SiO_2 interface. Both hole traps and electron traps may be present so that the net charge may be positive or negative. The oxide trapped charge is mainly due to impurities and structural defects. This charge can be created, for example, by X-ray radiation or high energy electron bombardment [25]. Unlike Dit and Q_f which can be modelled as a two dimensional charge sheet, the Q_{ot} exists three dimensionally in space. For this reason the charge density, the centroid and the capture cross section are also important parameters for the Q_{ot}. Several investigators [26,27,28] have studied these parameters by measuring the

current-voltage (I-V) characteristics with carriers injected into the oxide either by photo-injection or by avalanche injection. The oxide traps are generally shallow so that the trapping and detrapping of holes and electrons are relatively easy. The oxide trapped charge density can be reduced to the order of 10^{10} cm^{-2} by low temperature annealing in a forming gas.

The mobile ion charge is mainly caused by the presence of alkali metal ions such as K+ and Na+. Sodium ions are the most important ions because of their high mobility and their abundance in the environment. Mobile ions are normally introduced into the oxide as contaminants during the fabrication process and the metallization process, in which ions are trapped under the electrode and diffused into the oxide layer.

The mobile ion charge cannot be eliminated by annealing. The only way to reduce its concentration is to keep the fabrication system clean. A Si_3N_4 layer deposited on top of the SiO_2 layer before metallization may stop the diffusion of ions into the oxide layer. Once the ions reach the SiO_2-Si_3N_4 interface, they will be trapped there and become immobile. Typical values of the mobile ion charge density is about 10^{10} cm^{-2} for both the thermally grown oxide films and the PECVD oxide films.

2.4 Defective Models for the Si-SiO_2 interface

Modelling of the Si-SiO_2 interface region is essential for the development of the semiconductor technology. A good interface can provide important information for the oxidation process and better understanding of the origin and the nature of the defective charges. With these information, a better control of the properties of the Si-SiO_2 interface

could be developed. Several models have been proposed over the years and they are the coulombic, bond and defect models.

2.4.1 The Coulombic Model

This model first proposed by Goetzberger et al [29] suggest that the charge at the Si-SiO_2 interface is trapped by the potential wells induced by the oxide bulk charge. All oxide bulk charge within a distance D from the interface will give rise to the formation of surface states. D is assumed to be greater than two atomic layers and this idea is supported by two facts. First of all, due to the non-stoichiometric properties of the Si-SiO_2 interface, the number of positive charges and the number of negative charges would be unlikely the same in this region but the donor and acceptor states were found to be about the same. Secondly, if the oxide charge is located within one or two atomic layers from the Si-SiO_2 interface, the surface states will disappear due to the tunnelling of the oxide charge to the silicon. The existence time of an occupied surface state longer than 24 hours has been observed and this time is much longer than the expected tunnelling time. A schematic representation of the model is shown in Figure 2.8.

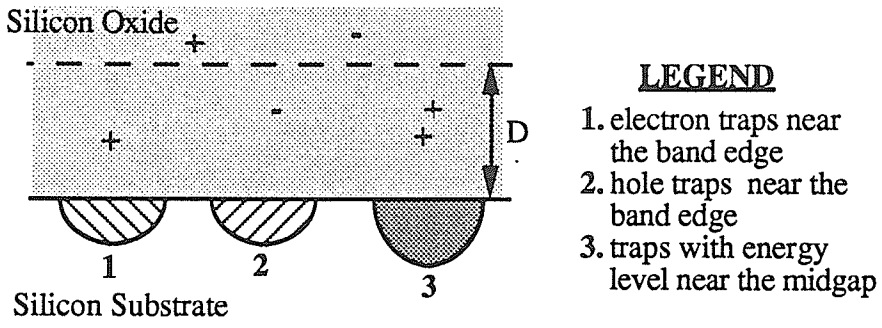

Figure 2.8: Schematic representation of the columbic model

Positive and negative oxide charges within the distance D with energy levels near the band edge give rise to the formation of electron and hole traps. Charge clusters in this region will also give rise to the formation of surface states with energy levels near the midgap. The number of charge clusters is obviously less than the number of single charge, and this would give rise to a U-shape distribution of the surface states. However, the predicted number of charge clusters is very low and thus give a much lower estimated midgap charge density than the experimental value.

2.4.2 The Bond Models

This model was first put forward by Sakurai and Sugano [30]. They calculated the energy levels for different surface bonding disorder models and found that the disorders are responsible for various energy levels. These disorders are probably caused by the strain and stress present at the Si-SiO_2 interface. A tight binding model for the silicon substrate with a Bathe lattice is shown in Figure 2.9.

Figure 2.9: Amorphous SiO_2 represented by a Bethe-lattice

Several models which energy levels was calculated is shown in Figure 2.10.

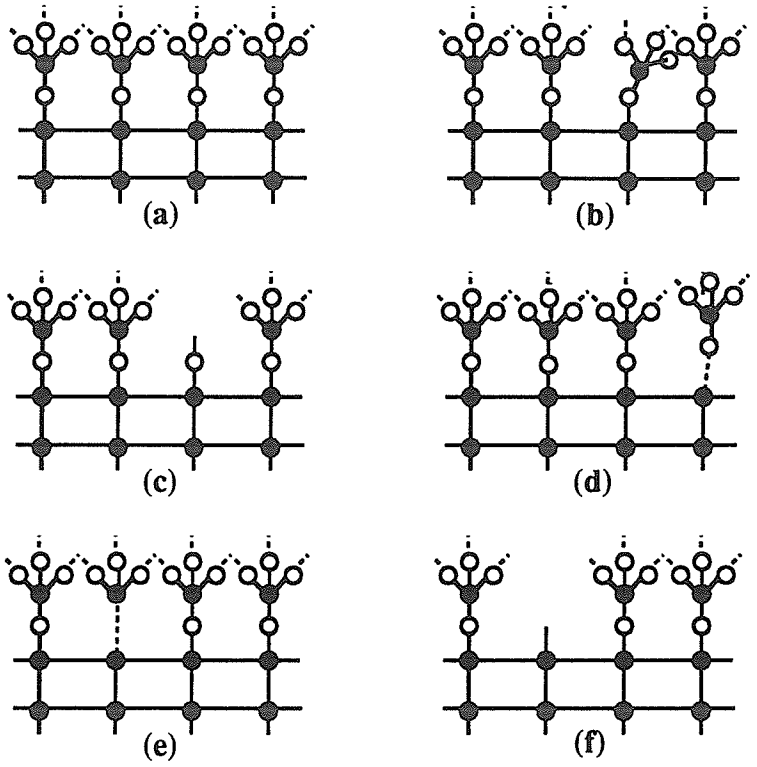

Figure 2.10: Several defect bond models, (a) perfect interface (b) with one of the bonds rotated, (c) oxygen dangling bond, (d)weak Si-O bond, (e) O-vacancy, and (f) Si dangling bond

A perfect interface is shown in Figure 2.10(a), the same structure but with one of the bonds rotated a certain angle is shown in Figure 2.10(b). Figure 2.10(c) shows an oxygen dangling bond with one of the tetrahedral structure missing and the oxygen bond unattached. For all of these structures, no energy level is found within 0.5 eV below the top of the valence band and 0.5 eV above the bottom of the conduction band. Therefore they have no contribution to the interface states. Figure 2.10(d) shows a weak Si-O bond with energy levels below the midgap of the silicon energy band gap. Figure 2.10(e) shows

a O-vacancy or a weak Si-Si bond with energy levels falling within the region above the midgap and below the conduction band. Both the Si-O weak bond and the Si-Si weak bond or O-vacancy will have the energy levels vary if the bond length or the bond angle is changed. At the Si-SiO_2 interface, these structures can come with various bond lengths and bond angles due to the local strain and stress, thus resulting in a continuous distribution of the energy levels. Figure 2.10(f) shows a Si dangling bond with energy levels around the middle of the energy gap. The Si dangling bond will be discussed in more detail in the following sections.

No reliable calculation for the density as a function of the energy levels is available. Furthermore, these models appear to be too simple to be realistic because the effect of the clustering of strained bonds and the interaction between them has not been taken into account.

2.4.3 The Defect Models

A more complete qualitative model is proposed by Nicollian and Brews [31]. They suggested that the Si-SiO_2 defects consist of stacking faults, micropores as well as various atomic or molecular fragments left behind after oxidation. Four types of defects are responsible for the creation of traps at the Si-SiO_2 interface. They are trivalent silicon (excess silicon), nonbridging oxygen (excess oxygen), impurities and oxide trapped charge. They are shown in Figure 2.11.

Upon all these defects, the most accepted defects as the interface traps are the silicon dangling bonds. They are probably formed due to the incomplete oxidation of silicon. It is a silicon atom with three of its four valence electrons bonded to neighboring atoms. The remaining electron can escape from the atom easily due to the low

electronegativity of the silicon atom and acts as a hole trap. Therefore it is positively charge when it captures a hole and neutral when empty.

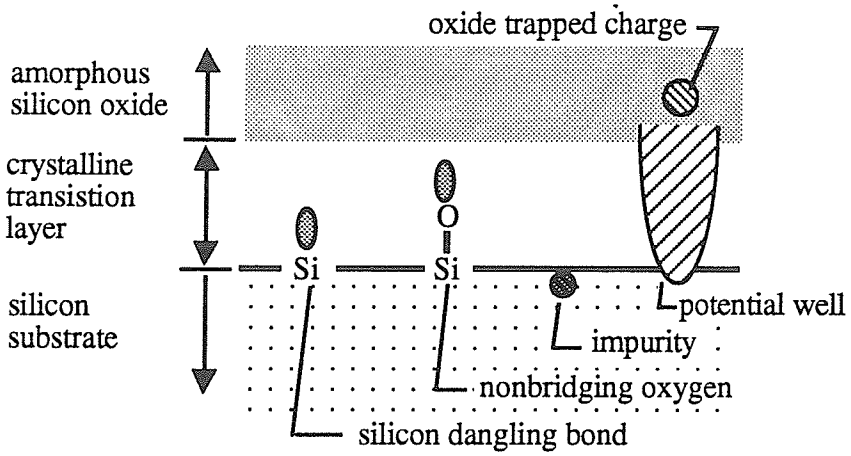

Figure 2.11: Defect model of the Si-SiO_2 interface

Nishi [32] and Poindexter [33] have reported that the signal from the electron paramagnetic resonance is related to the trivalent silicon, and the magnitude of this signal is proportional to the midgap interface density level. Therefore, they have concluded that there exist trivalent silicon at the Si-SiO_2 interface.

Nonbridging oxygen has not yet been identified as an electrical defect. Recently Rubloff [22] has reported that this defect could be formed by simply breaking a Si-O bond or by the presence of excess silicon atoms near the Si-SiO_2 interface which are left over after oxidation. The presence of this defect at the interface could release strain caused by the lattice mismatch between silicon structure and SiO_2 structure. The nonbridging oxygen atom shares one of its valence electrons with neighboring silicon atom and due to the high electronegativity of the oxygen atom, the remaining electron acts as an electron trap. Therefore it is negatively charged when it captures an electron and remains neutral when empty.

The strain at the interface creates a potential minimum for the impurities and therefore impurities tend to settle in this region. The impurities of the PECVD oxides may come from many external sources and therefore their trap densities are usually higher. However, for the conventional thermal oxides, these impurities mostly come from the dopants inside the silicon. For a silicon substrate with dopant concentration of $10^{15}cm^{-3}$, the amount of impurities at the Si-SiO_2 interface is about $10^{10}cm^{-2}$. This is probably the reason why there is a lower limit on the Si-SiO_2 interface trap density level. The fourth type of defects is the oxide trapped charge induced potential wells. This defect has been discussed earlier in section 2.4.1.

CHAPTER 3

NUMERICAL ANALYSIS OF THE ANNEALING PROCESSES

3.1 The Hydrogen Annealing Processes

The interface trapped charge and the oxide trapped charge can be minimized by thermal annealing in a forming gas in the last step of the fabrication process. The commonly used forming gas is a mixture of 10% to 25% of hydrogen in nitrogen gas. Annealing is normally performed at 400°C to 450°C for 10 to 45 minutes.

A great deal of previous works [34,35,36] on annealing have clearly delineated the importance of hydrogen in the annealing processes. It is generally believed that hydrogen is making its way to the Si-SiO_2 interface during annealing and reacts with the dangling bonds of silicon there, thus inhabiting those unsatisfied bonds to form traps. Some of the experimental facts that have puzzled investigators for years are:

(1) MOS devices with a polysilicon gate anneal much slower than those devices with an active metal gate, such as aluminum or magnesium.

(2) The speed of annealing is dependent on the lateral geometry for polysilicon gate devices, but not for aluminum gate devices.

(3) MOS devices with an active metal gate can be annealled even without hydrogen in the annealing ambient.

(4) Pre-metallization annealing of Si-SiO_2 interfaces proceeds more rapidly in hydrogen than in nitrogen.

These findings suggest that there are other hydrogen sources for annealing besides the forming gas, and that the annealing of active metal gate devices is not a straight forward process. Atomic hydrogen produced at the Al-SiO_2 interface is believed to be responsible for the annealing process in aluminum gate devices [12]. Aluminum reacts with the trace amount of water at the SiO_2 surface during metallization. The water at the SiO_2 surface is usually in the form of hydroxyl group and bonded to the SiO_2 surface as shown in Figure 3.1. It is the reaction between Al and the OH group at the metal-SiO_2 interface that produces atomic hydrogen.

$$Al + OH \rightarrow AlO + H \qquad (3.1)$$

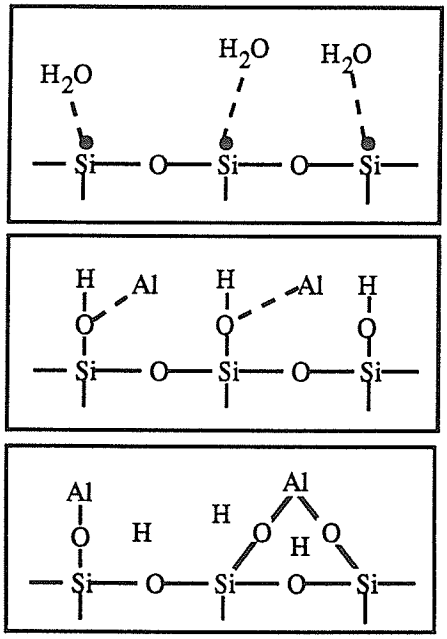

Adsorption of water molecules on the silicon surface
When silicon surface is exposed to air, the highly reactive silicon dangling bonds react with the moisture in the atmosphere to formOH groups. The water molecules do not react with the oxygen atoms on the surface because they are relatively stable.

Metalization
Aluminum atoms react with OH group
to produce atomic hydrogen

After metallization
Atomic hydrogen is generated and it is mobile. They diffuse to the silicon-silicon oxide interface and passivate the traps

Figure 3.1: The reaction of Al with the OH group leading to the generation of atomic H

The aluminum oxide is denoted by AlO instead of Al_2O_3 because the actual composition is not known and it probably changes during annealing.

The concentration of H is equal to the concentration of the hydroxyl groups at the Al-SiO_2 interface. This is about one-third of the total atomic concentration because the hydroxyl groups bond only to the silicon atoms but not to the oxygen atoms as shown in Figure 3.1. A schematic representation of the annealing processes is shown in Figure 3.2.

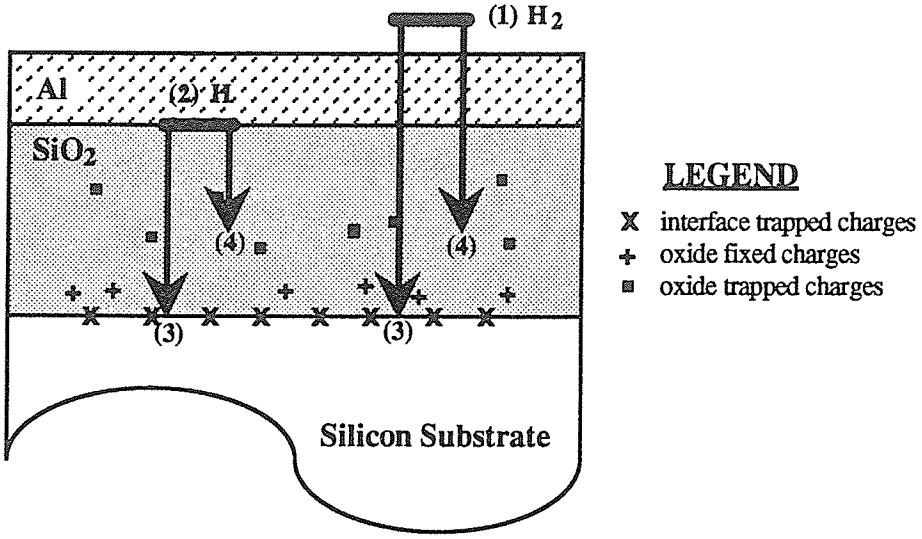

(1) The ambient is a source of molecular hydrogen for annealing.

(2) Al + OH $\rightarrow$ AlO + H is a source of atomic hydrogen for annealing.

(3) Hydrogen atoms and hydrogen molecules react with the interface traps and disables them from capturing carriers from the silicon substrate.

$$Si{\equiv}Si^{\bullet} + H \rightarrow Si{\equiv}Si\text{-}H$$

(4) Hydrogen atoms and hydrogen molecules react with the oxide traps to prevent it from capturing the tunneling electrons.

Figure 3.2: Illustrating the annealing processes

Hydrogen molecules dissociate into hydrogen atoms, thus reacting with the interface traps. This dissociation is probably catalyzed by the highly reactive interface traps. Besides the ambient and the metal-SiO interface which are acting as the sources of hydrogen, a third source may be the presence of H_2 inside the bulk of the PECVD oxide films. The reason of suggesting such a source is based on the fact that the reaction of SiH_4 with activated oxygen will produce hydrogen molecules which may be trapped inside the oxide layer during deposition. Although the Fourier Transform Infrared Spectrum (FTIR) does not

show any trace of hydrogen present inside the SiO_2 bulk, there is still a possibility that hydrogen may exist with a concentration under the detection limit of the FTIR which is about 0.5 to 1 atomic percent. In order words, the concentration of hydrogen up to 10^{20} cm^{-3}, cannot be detected but may be present in the SiO_2 bulk.

3.2 The Two Reaction Model

A single reaction model for interface trap annealing is based on the reaction between hydrogen atoms and the dangling bonds,

$$Si{\equiv}Si^{\bullet} + H \rightarrow Si{\equiv}Si\text{-}H \tag{3.2}$$

The differential equation corresponding to this reaction is

$$\frac{d}{dt}[Si^{\bullet}] = -k_1 \cdot [Si^{\bullet}] \cdot [H] \tag{3.3}$$

where $[Si^{\bullet}]$ and [H] are the surface concentrations of the silicon dangling bonds and hydrogen atoms, respectively. k_1 is the reaction rate constant and on the basis of the bimolecular reaction theory, it is given by

$$k_1 = 2 \cdot \pi \cdot \rho \cdot D_H \tag{3.4}$$

where ρ is the equivalent reaction radius and D_H is the diffusion coefficient of the mobile species, in this case hydrogen atoms. The solution to the above differential equation is

$$[Si^{\bullet}] = \frac{T_{ox}[H]_0 - [Si^{\bullet}]_0}{\{\frac{T_{ox}[H]_0}{[Si^{\bullet}]_0} \exp[(\frac{T_{ox}[H]_0 - [Si^{\bullet}]_0}{T_{ox}}) \cdot k_1 \cdot t] - 1\}} \tag{3.5}$$

where T_{ox} is the oxide thickness, $[Si^{\bullet}]_0$ is the original concentration of dangling bonds, and $[H]_0$ is the original concentration of hydrogen atoms. This reaction model has been found to be inaccurate because the solution of equation (3.4) does not fit the experimental data. Reed and Plummer [12] have suggested a two reaction model which fit the

experimental data much better than the single reaction model. The second reaction proposed by Reed and Plummer is

$$H + H \rightarrow H_2 \tag{3.6}$$

This equation describes the demerization of atomic hydrogen into molecular hydrogen (H_2). This reaction can occur readily due to two facts. One is the highly unstable atomic hydrogen tending to form more stable species such as H_2, and the other is the high mobility of atomic hydrogen providing a high reaction rate for this reaction and thus making it significant.

Although the fact that the interface traps can be passivated by the reaction with hydrogen is widely accepted, the actual mechanism of this process is still a mystery. The passivated traps are generally assumed to have the structure of SiH. So far, no conclusive results have been reported on the change of the concentration of Si-H before and after annealing. This has raised a question of whether any other path of reactions could have taken place such as hydrogen acting as a catalyst and not being consumed during the passivation process. Johnston et al. [37] have reported an increase of duterium accumulation at the Si-SiO_2 interface after annealing. This phenomenon is in favour of the consumptive mechanism but it could be due to the high stress at the interface which creates an energy minimum for the duterium and traps them. Until more conclusive results are found, both consumptive and non-consumptive reactions could be possible for the passivation mechanism, therefore both cases are briefly discussed in the following sections.

3.2.1 Theoretical Analysis for the Non-Consumptive Mechanism

The non-consumptive two reaction mechanism implies that the hydrogen atoms act as catalyst and are not consumed after the passivation reaction. At the same time, hydrogen atoms recombine to form molecular hydrogen inside the oxide bulk. The schematic representation of the model is shown in Figure 3.3.

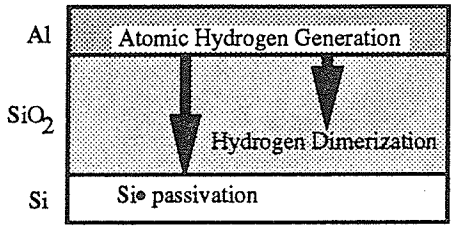

Figure 3.3: Schematic representation of the two reaction model

The two reactions can be described by

$$Si\bullet + H \rightarrow \oplus + H \tag{3.7}$$

$$H + H \rightarrow H_2 \tag{3.8}$$

The symbol $\oplus$ denotes a passivated trap center whose physical structure and chemical composition is unknown. It could be of the structure of tridymite or anything else. The only characteristic known is that this structure is electrically inactive. The corresponding differential equations for the reaction described in (3.7) and (3.8) are

$$\frac{d}{dt}[Si\bullet] = - k_1 \cdot [Si\bullet] \cdot [H] \tag{3.9}$$

$$\frac{d}{dt}[H] = -k_2 \cdot [H]^2 \tag{3.10}$$

where k_1 and k_2 are reaction rate constants for the passivation reaction (equation 3.7) and the dimerization reaction (equation 3.8), respectively. [Si•] and [H] are the concentrations

of the silicon dangling bonds and the hydrogen atoms at the Si-SiO_2 interface, respectively. Based on the chemical kinetic theory, k_1 and k_2 can be expressed as

$$k_1 = 2\cdot\pi\cdot\rho_1\cdot D_H \tag{3.11}$$

$$k_2 = 4\cdot\pi\cdot\rho_2\cdot D_H \tag{3.12}$$

where ρ_1 and ρ_2 are the sums of the reaction radii and are given by

$$\rho_1 = r_{Si} + r_H \tag{3.13}$$

$$\rho_2 = r_H + r_H \tag{3.14}$$

where r_{Si} and r_H are the capture cross section radii of silicon dangling bonds and hydrogen atoms, respectively. D_H is the diffusion coefficient of the hydrogen atoms, and it can be expressed empirically in the form of

$$D_H = D_0\cdot\exp\left(\frac{-E_H}{k\cdot T}\right) \tag{3.15}$$

where D_0 is the diffusion coefficient at T=0°K which is equal to $10^{-5}cm^{-2}s^{-1}$, and E_H is the activation energy for the diffusion of hydrogen atoms in silicon oxide which is about 0.75 eV [15]. The solution to equations (3.9) and (3.10) is

$$[Si\bullet] = \frac{[Si\bullet]_0}{\{1 + 2\cdot k_2\cdot[H]_0\cdot t\}^{\eta}} \tag{3.16}$$

where $[Si\bullet]_0$ and $[H]_0$ is the initial concentrations of silicon dangling bonds and hydrogen atoms at the Si-SiO_2 interface, respectively; t is the annealing time and

$$\eta = \frac{k_1}{2\cdot k_2} \tag{3.17}$$

The radius of a hydrogen atom is 0.5Å. The capture cross section of the trivalently bonded silicon atom is not known but it is assumed to be at least as large as the radius of the silicon tetrahedral radius which is about 1.2Å, and may be up to 50% larger which is then 1.8Å. The initial concentration of the silicon dangling bonds ($[Si\bullet]_0$) can be found by experimental method only. In our case, ECR PECVD oxides of 200Å in thickness were

deposited on silicon substrates inside the plasma chamber with deposition parameters given in appendix A. An aluminum layer was deposited onto the oxide surface to form the gate electrode for the MOS device. The high-low frequency capacitance-voltage method was used to extract the Si-SiO_2 interface information. A Booton 72AD was used for measuring the high frequency C-V characteristics and a HP 4140b pA meter was used for measuring the quasi static C-V characteristics. The data was then fed into a computer program for the calculation of the initial silicon dangling bond density and the interface trap density. The computer program is given in Appendix B. Five MOS capacitors were used for each case to ensure the consistency of the experimental results. The capacitors were then annealed in forming gas containing 10% H_2 at 400°C for a predetermined time. The characterization procedure was repeated each time until the accumulated annealing time of 3600 seconds was reached. These interface trap density data were used as the experimental references for the numerical analysis. The initial value of the atomic hydrogen $[H]_0$ depends very much on the reaction between the gate aluminum and the traces of water as described in Section 3.1, the oxide thickness and the amount of OH groups. The following assumptions have been made [12].

(1) The amount of OH groups is sufficient for the reaction,

(2) the gate aluminum reacts efficiently with the OH groups within the temperature range under this investigation, and

(3) the transport of atomic hydrogen through the oxide is not the rate limiting process in the annealing processes.

The initial concentration of hydrogen atoms $[H]_0$ can be estimated by

$$[H]_0 = N_{OH} \cdot \exp\left(\frac{-E_R}{kT}\right) \tag{3.18}$$

where N_{OH} is the concentration of OH groups on the metal-silicon oxide interface and it has been estimated to be 1.67×10^{23} cm^3 [12]. E_R is the activation energy for the reaction which is assumed to be 0.46eV. Therefore $[H]_0$ is estimated to be $6 \times 10^{19} cm^{-3}$. Using these initial values and equation (3.16), the capture cross section of the silicon dangling bond is found to be 1.62Å which is within the estimated value of 1.2Å to 1.8Å [38].

The non-consumptive mechanism of the two reaction model is the simplest case of our interest and it is the only case which can be solved analytically. Later, we shall present other reaction models which are more complicated and the differential equations used to described them cannot be solved analytically. The only way to solved them is to use numerical methods.

3.2.2 Numerical Analysis for the Non-Consumptive Mechanism

Since all the annealing models are evaluated by a numerical simulation method, it is worthy to find out the validity of the method by comparing it to a model for which analytical results are available. The non-consumptive two reaction model is a perfect candidate for such a comparison since it is the only model for which analytical results are available.

The numerical method employed to solve the differential equations is the Adams-Moulton method. It is a multi-step method consisting of two equations, one is the predictor equation and the other is the corrector equation and they are

Predictor:
$$y_{n+1} = y_n + \frac{h}{24}(55f_n - 59f_{n-1} + 37f_{n-2} - 9f_{n-3}) \tag{3.19}$$

Corrector:
$$y_{n+1} = y_n + \frac{h}{24}(9f_{n+1} + 19f_n - 5f_{n-1} + f_{n-2}) \tag{3.20}$$

where f is the first derivative of y which is the differential equation to be solved. The predictor is a cubic polynomial which is used to fit the data to get a new value for the derivative f_{n+1}. This value is integrated together with three previous derivative data to get a new data point y_{n+1}. This method is faster and simpler as compared to other numerical methods because for this method only two calculation steps are necessary. This is the reason why it is more favorable than other methods. It has an error which is proportional to the fifth power of the step size, and this is acceptable in our analysis.

The only short coming of this method is that four data points are needed to start the calculation but only one initial data point is available experimentally. Therefore the Runge-Kutta algorithm has to be employed for the generation of the first four data points. Four intermediate derivative points are used to estimate a new data point, one at the position of the presently known data point, one at the position of the predicting data point and twice in the middle of the two. These four intermediate derivatives are then integrated over the step size to yield the new data. The equations used are given below:

$$y_{n+1} = \frac{1}{6}(k_1 + 2\cdot k_2 + 2\cdot k_3 + k_4) \tag{3.21}$$

where

$$k_1 = h\cdot f(x_n, y_n) \tag{3.22}$$

$$k_2 = h\cdot f(x_n + \frac{k_1}{2}, y_n + \frac{k_1}{2}) \tag{3.23}$$

$$k_3 = h\cdot f(x_n + \frac{k_2}{2}, y_n + \frac{k_2}{2}) \tag{3.24}$$

$$k_4 = h\cdot f(x_n + k_3, y_n + k_3) \tag{3.25}$$

This is a suitable choice for estimating the four initial points because it also has an error proportional to the fifth power of the step size which is the same as that for the Adams-Moulton method.

The two algorithms are used together to simulate the model with the dangling bond capture cross section radius as a varying parameter. The best fit is decided by the

minimization of an error term. Since the interface trap density depends exponentially on time, simply adding the differences between the experimental data and the simulation data together based on equation (3.26) would create a bias that the first few data points have more effect on the error term than the rest.

$$\text{error} = \sum | d_{\text{experimental}} - d_{\text{simulated}} | \tag{3.26}$$

This can be seen more clearly in Figure 3.4

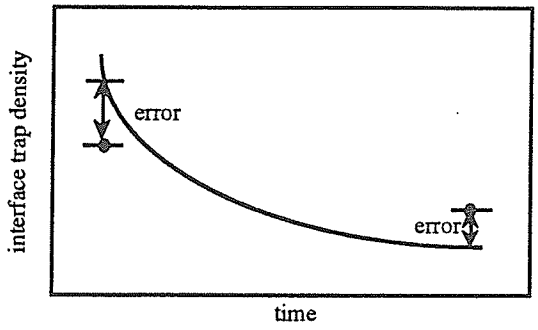

Figure 3.4: The bias of the error towards large trap density region

Special care has to be taken for the calculation of the error term in order to eliminate the bias. Taking natural log of all the data points could make all the data points to fall into the same order and reduce the bias but the bias is still observable. Reed et al [12] have estimated the best simulation fit by using the least square method, that is by adding the square of the differences between the experimental data and the simulated data as given by

$$\text{error} = \sum (d_{\text{experimental}} - d_{\text{simulated}})^2 \tag{3.27}$$

This method can provide absolute values of the differences but it cannot eliminate the bias at all. The best way to eliminate the bias is to use the percentage error method as given by

$$\text{error} = \sum \left(\frac{|\Delta d|}{d_{\text{experimental}}} \right) \tag{3.28}$$

This method is simple and require minimal amount of computation time and therefore a suitable candidate for the estimation of the validity of the models. By using the method described above, a computer simulation is done by using a program written in Lightspeed Pascal on a Macintosh SE/30 for the non-consumptive two reaction model.

The trap densities at different times are calculated with the radius of the silicon dangling bonds capture cross section assumed to be 1.2, 1.7 and 2.2Å. Th results are shown in Figure 3.5(a) and those for the corresponding [H] shown in Figure 3.5(b). It can be seen that the simulation results are in reasonable agreement with the experimental data. The calculated values of the error term with respect to the silicon dangling bond capture cross sections are shown Figure 3.6.

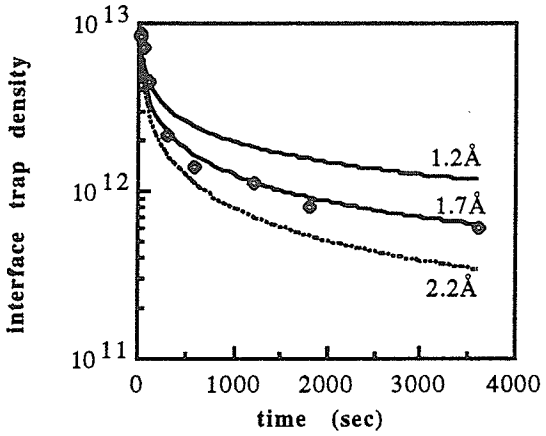

Figure 3.5(a): Simulation results of the values of D_{it} for three dangling bond capture cross sections

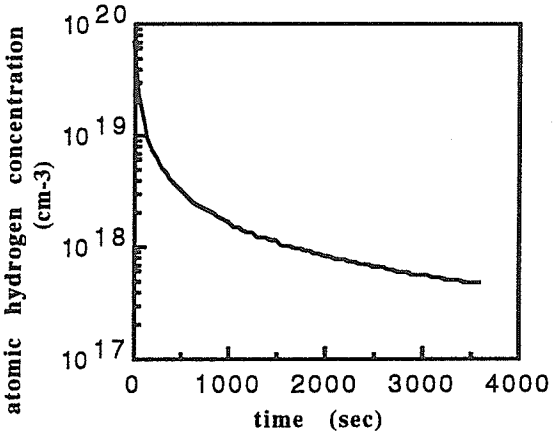

Figure 3.5(b): Simulation results of atomic hydrogen concentration inside the oxide bulk

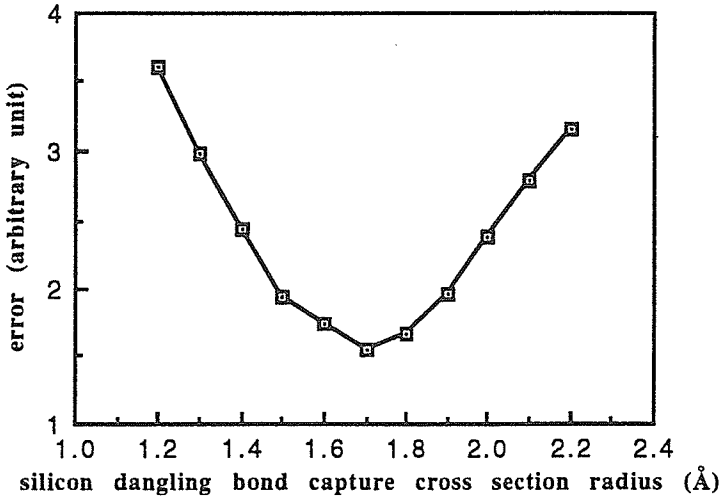

figure 3.6: Computed value of the error term as a function of the silicon dangling bond capture cross section radius

Figure 3.6 shows that the best fit is obtained when the radius of the silicon dangling bond capture cross section is about 1.6 - 1.7Å. This agrees well with the theoretical estimation mentioned in section 3.2.1, suggesting that this simulation method is acceptable for the computation of the capture cross section radius.

3.2.3 The Consumptive Two Reaction Model

The consumptive two reaction model consists of a passivation reaction and a hydrogen dimerization reaction. The only difference from the non-consumptive model is that the hydrogen atoms are consumed in the reaction with the silicon dangling bonds forming Si-H as the end product. The two reactions of the consumptive models are

$$Si\bullet + H \xrightarrow{k1} SiH \tag{3.29}$$

$$H + H \xrightarrow{k2} H_2 \tag{3.30}$$

The corresponding differential equations are

$$\frac{d}{dt}[Si\bullet] = -k_1 \cdot [Si\bullet] \cdot [H] \tag{3.31}$$

$$\frac{d}{dt}[H] = -k_1 [Si\bullet] \cdot [H] - 2 \cdot k_2 \cdot [H]^2 \tag{3.32}$$

where k_1 and k_2 are reaction constants which can be expressed in the form of equations (3.11) and (3.12), respectively. The extra term presence in equation (3.32), by comparing with equation (3.10) is due to hydrogen atoms being consumed at a rate of k_1 while reacting with silicon dangling bonds.

Utilizing the error estimation method described in section 3.2.2 and equation (3.28), the value of the error term as a function of the silicon dangling bond capture cross section radius is shown in figure 3.7. It can be seen that the best fit occurs when the radius of the silicon dangling bond is about 1.6 to 1.7Å. This finding is very close to that based

on the non-consumptive two reaction model. This may imply that the amount of hydrogen atoms consumed through the passivation reaction is insignificant compared to the amount that is consumed by the dimerization reaction. Therefore, equation (3.32) can be simplified by ignoring the $k_1 \cdot [Si\bullet] \cdot [H]$ term which reduce it to equation (3.10). This makes the differential equations to be exactly the same as those for the non-consumptive two reaction model, and therefore they yield the same results. In later sections, the non-consumptive and consumptive models will be discussed simultaneously since they are likely to yield similar results.

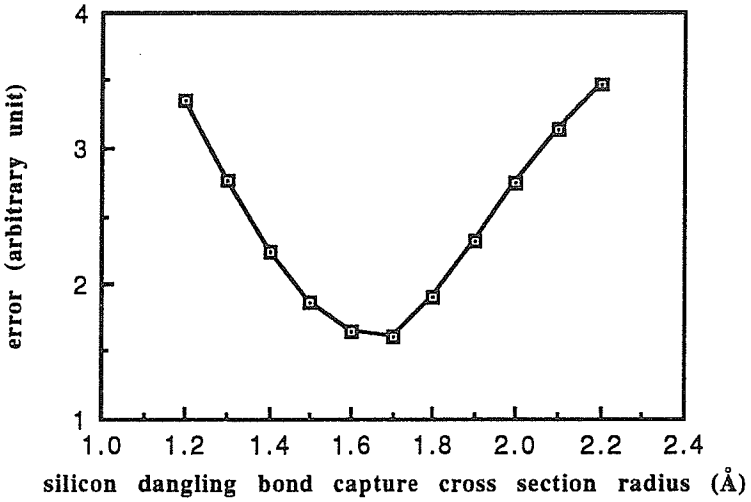

Figure 3.7: Computed value of the error term as a function of the silicon dangling bond capture cross section

3.3 The Three Reaction Model (Including H_2)

It has been shown by many investigators that the interface trap density of Si-SiO_2 systems without an active metal electrode (This case will be referred to as bare oxide) can be reduced by annealing in an ambient containing hydrogen gas. Without the active metal electrode, the process described in section 3.1 which generates hydrogen atoms does not exists and no atomic hydrogen should be produced. Without atomic hydrogen, the

passivation reaction described by the two reaction model could not proceed and therefore the interface trap density should remain constant. This is in contradiction to the experimental results shown in Table 3.1. This suggests that the two reaction model cannot completely describe the annealing processes. Another experimental fact which has to be taken into account is that the interface trap density of a bare oxide cannot be reduced at all when annealed in a hydrogen free medium [10], implying the importance of the presence of hydrogen.

Table 3.1: Experimental facts indicating the importance of H_2 in the annealing processes

ambient	with electrodes	no electrodes
N_2	annealed	not annealed
H_2 in N_2	annealed	annealed

It is likely that hydrogen molecules from the environment can somehow work their way through the oxide bulk to the Si-SiO_2 interface and react with the interface traps thus passivating them. If this is true, then the two reaction model does not describe completely the annealing processes because it does not includes the reaction of the interface traps with hydrogen molecules which is believed to be the passivation mechanism for the annealing of bare oxides in a medium containing hydrogen molecules. We therefore propose a three reaction model including the reaction between hydrogen molecules and silicon dangling bonds. For the non-consumptive case, this reaction can be written as

$$Si\bullet + H_2 \rightarrow \oplus + H_2 \tag{3.33}$$

Similarly, for the consumptive case, it can be written as

$$Si\bullet + H_2 \rightarrow SiH + H \tag{3.34}$$

The non-consumptive mechanism three reaction model is shown schematically in Figure 3.8.

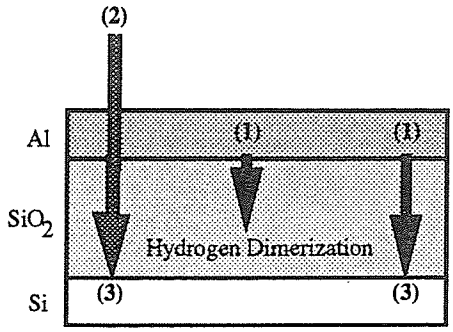

Figure 3.8: Schematic representation of the three reaction model

The three reactions for this model can be written as

$$Si\bullet + H \xrightarrow{k1} \oplus + H \tag{3.35}$$

$$Si\bullet + H_2 \xrightarrow{k2} \oplus + H_2 \tag{3.36}$$

$$H + H \xrightarrow{k3} H_2 \tag{3.37}$$

Equation (3.36) is very unlikely to be a fundamental equation. The actual reaction could be in the following sequence

$$(1) \quad Si\bullet + H_2 \rightarrow \oplus\text{-}H + H \tag{3.38}$$

$$(2) \quad \oplus\text{-}H + H \rightarrow \oplus + H_2 \tag{3.39}$$

This is just an assumption and no direct proof is yet available for the actual mechanism. This assumption does not affect the reaction rate as long as reaction (2) is not the rate limiting reaction. From equations (3.35) to (3.37), the corresponding differential equations are

$$\frac{d}{dt}[Si\bullet] = -k_1\cdot[Si\bullet]\cdot[H] - k_2\cdot[Si\bullet]\cdot[H_2] \tag{3.40}$$

$$\frac{d}{dt}[H] = -2\cdot k_3\cdot[H]^2 \tag{3.41}$$

$$\frac{d}{dt}[H_2] = k_3\cdot[H]^2 \tag{3.42}$$

where

$$k_1 = 2\cdot\pi\cdot\rho_1\cdot D_H \quad (3.43)$$

$$k_2 = 2\cdot\pi\cdot\ \rho_2\cdot D_{H_2} \quad (3.44)$$

$$k_3 = 4\cdot\pi\cdot\rho_3\cdot D_H, \quad (3.45)$$

D_{H_2} is the diffusion coefficient of molecular hydrogen and

$$\rho_1 = r_{Si} + r_H \quad (3.46)$$

$$\rho_2 = r_{Si} + r_{H_2} \quad (3.47)$$

$$\rho_3 = r_H + r_H \quad (3.48)$$

Equations (3.40) to (3.42) together with the error estimation method are used for the evaluation of the validity of this model. The simulation results show that the differential equations are not converging and yield unreasonable results for the [Si•]. The differential equations have been reviewed together with the concentrations of hydrogen atoms and hydrogen molecules inside the bulk taken into account. The $[H_2]$ in the oxide bulk raise rapidly due to the demerization of hydrogen atoms and reach a concentration in the order of 10^{19} cm^{-3}. This is expected but the problem arise when hydrogen molecules can react with silicon dangling bonds. This increases the passivation rate of the silicon dangling bonds by two orders and it is the major reason why the computed results are unreasonable.

The reason behind this which cause the unexpectedly high passivation rate of the silicon dangling bonds is the incorrect estimation of the reaction rate constant for the reaction between hydrogen molecules and the dangling bonds, k_2. The calculation of k_2 by equation (3.44) is in an incorrect form because this equation is based on the assumption that hydrogen molecules can react with the dangling bonds at an activation energy of zero. It is obvious that this assumption is incorrect. This is due to the fact that the hydrogen molecules have to dissociate into two hydrogen atoms somehow in the passivation process as described in equations (3.38) and (3.39). To take this factor into account, the

expression for k_2 has to be modified by multiplying it to an exponential term and change it to the form of an Arrhenius equation. The new equation is thus

$$k_2 = 2\cdot\pi\cdot\rho\cdot D_{H_2}\cdot\exp\left(\frac{-E_{Si}}{k\cdot T}\right) \tag{3.49}$$

where E_{Si} is the activation energy for the reaction between hydrogen molecules and the dangling bonds, k is the Boltzman constant and T is the absolute temperature. Since the activation energy for this reaction is unknown and therefore it is also treated as a variable parameter. Together with the variation of the capture cross section of the dangling bonds, the computed values of the error term as a function of the silicon dangling bond activation energy is shown in Figure 3.9.

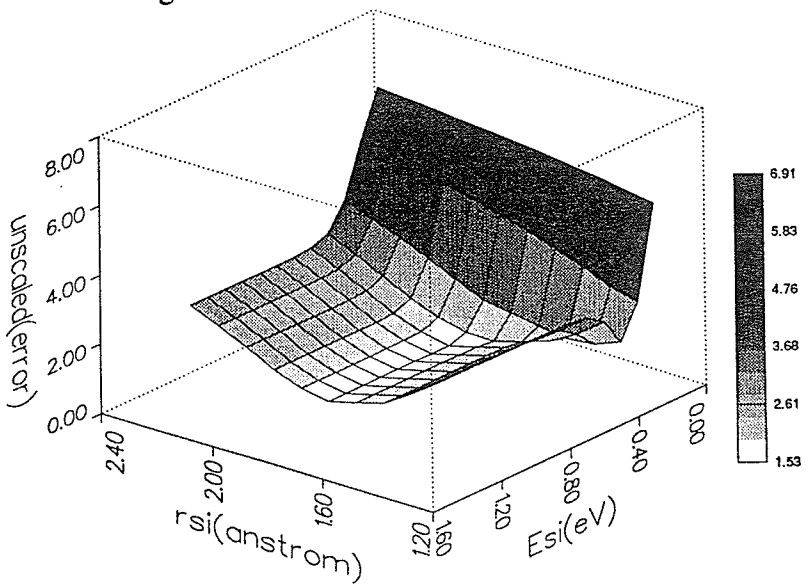

Figure 3.9: Computed value of the error term as a function of the silicon dangling bond capture cross section radius and the activation energy E_{Si}

It can be seen that as the activation energy (E_{Si}) approaches zero, the value of the error term increases very rapidly, and this is where the non converging results occur. The values of the error term fall into a reasonable region for E_{Si} larger than 0.4eV. This means that the reaction between hydrogen molecules and dangling bonds requires a certain amount of activation energy as expected. In fact, the best fit to the experimental data points is

obtained when the E_{Si} is about 0.6eV. It can also be seen that the best fit also occurs when the capture cross section radius of the dangling bond is about 1.6Å. This agrees well with the results found in section 3.2 for the two reaction models. The computed value of the error term as a function of the activation energy is shown in Figure 3.10.

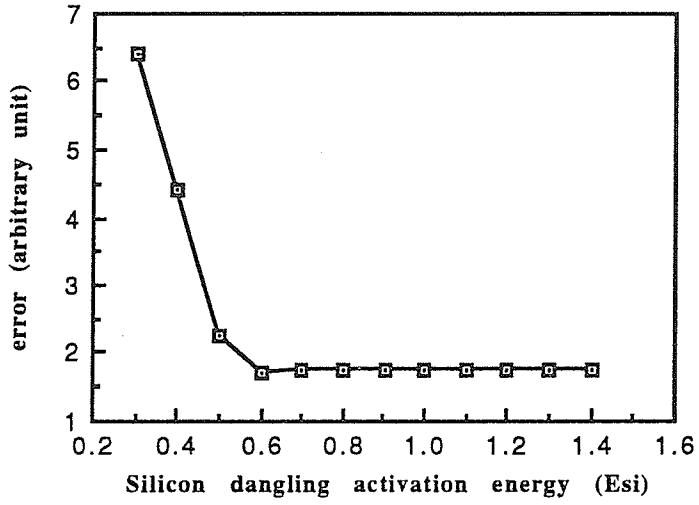

Figure 3.10: The computed value of the error term as a function of the activation energy E_{Si}

There is a minimum in E_{Si} equal to 0.6eV and for E_{Si} greater than 0.7eV, the values of the error term became almost constant. The reason is that for larger E_{Si}, the reaction rate constant (k_2) which is inversely proportion to the exponential of E_{Si} will becomes zero and all differential equations for the three reaction model will reduce to the same as those for the two reaction model. It is also found that the error term levels off very close to the activation energy where the best fit occurs. The reason is that the rate of the reaction between the hydrogen molecules and the dangling bonds is much slower than the rate hydrogen atoms and the dangling bonds. This can be seen that k_2 is close to zero as compared to k_1 for E_{Si} equal to 0.6eV. If k_2 is larger than k_1, then the error term would rise again before it levels off.

The consumptive three reaction model is similar to the corresponding non-consumptive one except that hydrogen are being consumed in the reactions. A schematic description is similar to the one shown in figure 3.9 but the reactions for this model become

$$Si\bullet + H \xrightarrow{k_1} SiH \tag{3.50}$$

$$Si\bullet + H_2 \xrightarrow{k_2} SiH + H \tag{3.51}$$

$$H + H \xrightarrow{k_3} H_2 \tag{3.52}$$

and the corresponding differential equations become

$$\frac{d}{dt}[Si\bullet] = -k_1\cdot[Si\bullet]\cdot[H] - k_2\cdot[Si\bullet]\cdot[H_2] \tag{3.53}$$

$$\frac{d}{dt}[H] = -k_1\cdot[Si\bullet]\cdot[H] + k_2\cdot[Si\bullet]\cdot[H] - 2\cdot k_3\cdot[H]^2 \tag{3.54}$$

$$\frac{d}{dt}[H_2] = -k_2\cdot[Si\bullet]\cdot[H_2] + k_3\cdot[H]^2 \tag{3.55}$$

The expressions for k_1 and k_3 are the same as those given in equations (3.43) and (3.45), and k_2 takes the form given in equation (3.49) for which the activation energy is taken into account for a more accurate model.

The same procedure used for the non-consumptive model has been carried out for the consumptive one with the activation energy and the dangling bond capture cross section radius as varying parameters. The values of the error term calculated for the consumptive model are similar to those for the non-consumptive one, and the minimum error value occurs when the activation energy is 0.6eV and the dangling bond capture cross section radius is 1.6Å. These results also agrees well with the previous findings. The reason that the consumptive model and the non-consumptive model behave similarly is probably due to the amount of atomic and molecular hydrogen consumed is negligible as compared to their total concentrations.

Due to the slow reaction rate between the hydrogen molecules and the dangling bonds, this reaction alone may not be enough for creating a noticeable effect in the annealing of bare oxides in the ambient containing hydrogen gas. However, no conclusion about this can be made at this point. Further experiments such as the dependence of the annealing time for the bare oxide in forming gas is needed to prove whether this reaction alone is sufficient or not. If the result is negative, there is a possibility that the molecular hydrogen may somehow be dissociated into atomic hydrogen inside the oxide bulk on its way to the Si-SiO_2 interface. Of course, if molecular hydrogen is dissociated into atomic hydrogen, the reaction rate should be increased.

One point that is made clear from this simulation is that there is indeed a reaction between the molecular hydrogen and the silicon dangling bonds and this explains at least partially why bare oxide can be annealed in the forming gas.

3.4 Three Reaction Models (Including SiO)

Another issue which has to be addressed in modelling the Si-SiO_2 interface is the physical nature of the interface traps. So far in this thesis, the interface traps are assumed to be of the nature of the silicon dangling bonds. In this section, we shall discuss the actual composition of the interface traps.

Rubloff [22] have suggested that there is a three stage process for the evolution of the interface traps. In this model, SiO_2 reacts with Si to form SiO which is the suspected candidate for the second kind of interface traps. Aspens and Theeten [21] have also shown that the chemical composition of the Si-SiO_2 interface is a chemical mixture of silicon and oxygen with a ratio of $SiO_{0.4}$. This suggests that the possibility for the presence of SiO defects at the interface cannot be ruled out. In this section, a three reaction model with SiO

together with Si• as the interface defects is presented. For simplicity, only atomic hydrogen is considered for the time being and the models including both SiO and H_2 will be presented in the next section.

This three reaction model for the non-consumptive case is shown schematically in Figure 3.11.

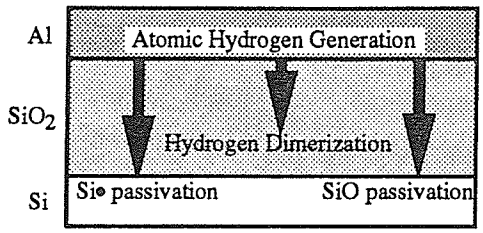

Figure 3.11: Schematic representation of the reaction model with SiO

The three reactions are

$$SiO + H \xrightarrow{k_1} \otimes + H \tag{3.56}$$

$$Si\bullet + H \xrightarrow{k_2} \oplus + H \tag{3.57}$$

$$H + H \xrightarrow{k_3} H_2 \tag{3.58}$$

where $\otimes$ and $\oplus$ are unknown structures which are electrically inactive. The corresponding differential equations are

$$\frac{d}{dt}[SiO] = -k_1 \cdot [SiO] \cdot [H] \tag{3.59}$$

$$\frac{d}{dt}[Si\bullet] = -k_2 \cdot [Si\bullet] \cdot [H] \tag{3.60}$$

$$\frac{d}{dt}[H] = -2 \cdot k_3 \cdot [H]^2 \tag{3.61}$$

where k_1, k_2 and k_3 are the reaction constants which are given by

$$k_1 = 2 \cdot \pi \cdot \rho_1 \cdot D_H \tag{3.62}$$

$$k_2 = 2\cdot\pi\cdot \rho_2\cdot D_H \tag{3.63}$$

$$k_3 = 4\cdot\pi\cdot\rho_3\cdot D_H \tag{3.64}$$

and ρ_1, ρ_2, ρ_3 are given by

$$\rho_1 = r_{SiO} + r_H \tag{3.65}$$

$$\rho_2 = r_{Si} + r_H \tag{3.66}$$

$$\rho_3 = r_H + r_H \tag{3.67}$$

For the consumptive variation of this model, the reactions are very similar and they can be written as

$$SiO + H \xrightarrow{k_1} SiOH \tag{3.68}$$

$$Si\bullet + H \xrightarrow{k_2} SiH \tag{3.69}$$

$$H + H \xrightarrow{k_3} H_2 \tag{3.70}$$

The corresponding differential equations are

$$\frac{d}{dt}[SiO] = -k_1\cdot[SiO]\cdot[H] \tag{3.71}$$

$$\frac{d}{dt}[Si\bullet] = -\,k_2\cdot[Si\bullet]\cdot[H] \tag{3.72}$$

$$\frac{d}{dt}[H] = -k_1\cdot[SiO]\cdot[H] - k_2\cdot[Si\bullet]\cdot[H] - 2\cdot k_3\cdot[H]^2 \tag{3.73}$$

where k_1, k_2 and k_3 are the same as those given in equations (3.62) - (3.64).

Since the initial ratio of the density of Si• to the density of SiO is unknown, therefore it is treated as an unknown parameter when performing the simulation computation. The percentage of the SiO defects in the total number of traps is expected to be in the order of a few percent. This is due to the fact that no electron paramagnetic resonance (EPR) signal besides that of the silicon dangling bonds has been reported. If the concentration of SiO defects is at a high percentage, this can probably be observed in the EPR signals.

The capture cross section radius of the SiO defects is also not known and it is assumed to be the sum of the radii of the tetrahedral silicon and oxygen which is about 1.84Å. The validity of this assumption will be verified later in this section. The activation energies for the reactions between atomic hydrogen and both defect structures are assumed to be very low and therefore the rates for the reactions shown in equations (3.62) and (3.63) are valid.

The simulation results with the capture cross section radius of silicon dangling bonds and the Si•/SiO ratio as varying parameters are shown in figure 3.12.

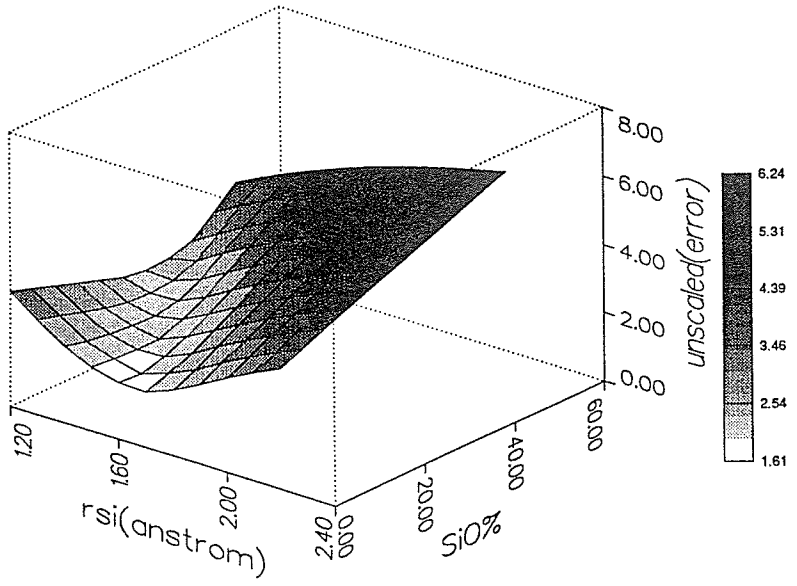

Figure 3.12: Computed value of the error term as a function of the silicon dangling bond capture cross section radius and the SiO/Si• ratio

It can be seen that the error term has its minimum at the point where the capture cross section radius of the silicon dangling bond is 1.6Å and the SiO is 5% of the total number of traps. The error as a function of the SiO/Si• with the capture cross section radius dangling bond set to 1.6Å is shown in Figure 3.13.

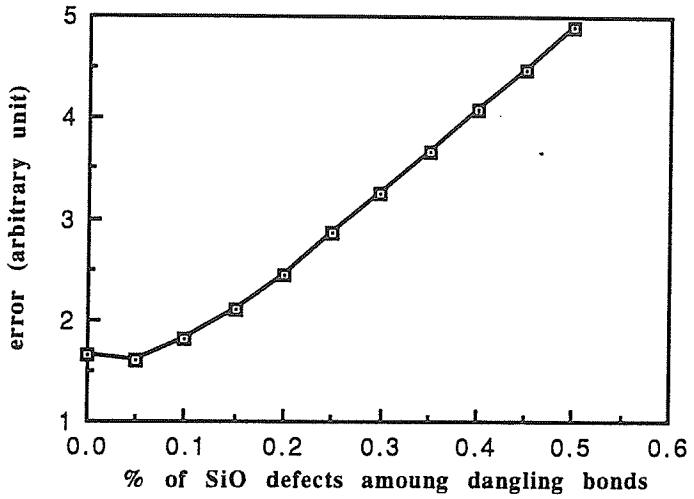

Figure 3.13: Computed value of the error term as a function of the SiO/Si• ratio

It can be seen more clearly that the minimum value of the error term is at the point where SiO is 0.05 of the total number of traps. However, at the point where SiO does not exist is also a reasonable approximation. =The value of the error term increases with the increasing concentration of SiO defects because the SiO has a larger capture cross section radius and thus speed up the passivation rate of the interface traps. The same explanation could be applied for the capture cross section radii of the silicon dangling bonds above 1.6Å. The value of the error term increases as the capture cross section radius of the dangling bonds decreases when it is below 1.6Å. This is due to the small capture cross section which tends to slow down the reaction rate.

Another unknown parameter which has to be considered is the capture cross section radius of the SiO. The following simulation is done with the capture cross section radius of silicon dangling bond set to be 1.6Å and with the capture cross section radius of SiO and the SiO percentage as varying parameters. The results are shown in Figure 3.14.

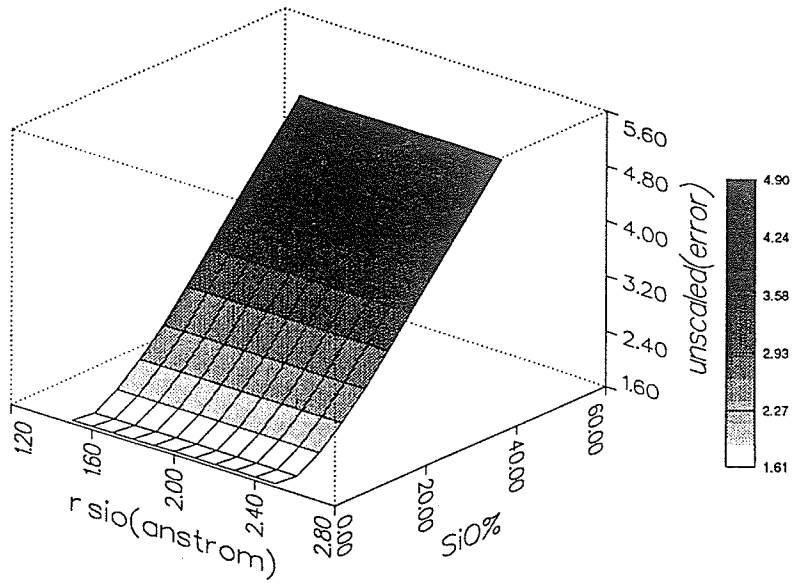

Figure 3.14: Computed value of the error term as a function of the SiO defect capture cross section radius and the SiO/Si• ratio

Simulation computation has been performed with the capture cross section radii of the SiO between 1.5Å and 2.5Å. This is a reasonable range for the actual value because the SiO structure is larger as compared to the silicon dangling bond. It can be seen from Figure 3.14 that the value of the error term is not sensitive to the change of the SiO capture cross section radius. This could be due to the fact that the percentage of SiO in the interface traps is very low. Therefore it does not affect the value of the error term by a significant amount in the range of radii which is of our interest.

The results from the consumptive variation of this model are very similar to those for the non-consumptive model. These results also agree well with previous findings and theoretical predictions and thus the reaction model with SiO is a reasonable model for explaining the annealing processes.

3.5 The Multi-Reaction Model with SiO and H_2

The model presented in the previous section suggested that the presence of SiO defects at the Si-SiO_2 interface is probable. One drawback of such model is that it has the same deficiency as the two reaction model. In order to make it satisfactory concerning the bare oxide annealing processes, the reaction with molecular hydrogen is also included. A schematic representation of the newly proposed multi-reaction model is shown in Figure 3.15

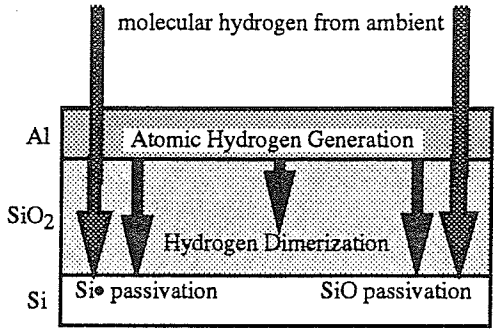

Figure 3.15: Schematic representation of the multi-reaction model

The reactions for the non-consumption case of this model can be written as

$$\mathrm{Si}\bullet + \mathrm{H} \xrightarrow{k_1} \oplus + \mathrm{H} \tag{3.74}$$

$$\mathrm{Si}\bullet + \mathrm{H_2} \xrightarrow{k_2} \oplus + \mathrm{H_2} \tag{3.75}$$

$$\mathrm{SiO} + \mathrm{H} \xrightarrow{k_3} \otimes + \mathrm{H} \tag{3.76}$$

$$\mathrm{SiO} + \mathrm{H_2} \xrightarrow{k_4} \otimes + \mathrm{H_2} \tag{3.77}$$

$$\mathrm{H} + \mathrm{H} \xrightarrow{k_5} \mathrm{H_2} \tag{3.78}$$

Equations (3.75) and (3.77) are probably not fundamental reactions as discussed in section 3.3. They probably go through some set of reactions similar to those described by equations (3.38) and (3.39). The corresponding differential equations are

$$\frac{d}{dt}[Si\bullet] = -k_1\cdot[Si\bullet]\cdot[H] - k_2\cdot[Si\bullet]\cdot[H_2] \tag{3.79}$$

$$\frac{d}{dt}[SiO] = -k_3\cdot[SiO]\cdot[H] - k_4\cdot[SiO]\cdot[H_2] \tag{3.80}$$

$$\frac{d}{dt}[H] = -\,2\cdot k_5\cdot[H]^2 \tag{3.81}$$

$$\frac{d}{dt}[H_2] = k_5\cdot[H]^2 \tag{3.82}$$

where

$$k_1 = 2\cdot\pi\cdot\rho_1\cdot D_H \tag{3.83}$$

$$k2 = 2\cdot\pi\cdot\rho_2\cdot D_H\cdot\exp\left(\frac{-E_{Si}}{k\cdot T}\right) \tag{3.84}$$

$$k_3 = 2\cdot\pi\cdot\rho_3\cdot D_H \tag{3.85}$$

$$k4 = 2\cdot\pi\cdot\rho_4\cdot D_H\cdot\exp\left(\frac{-E_{SiO}}{k\cdot T}\right) \tag{3.86}$$

$$k_5 = 4\cdot\pi\cdot\rho_5\cdot D_H \tag{3.87}$$

and

$$\rho_1 = r_{Si} + r_H \tag{3.88}$$

$$\rho_2 = r_{Si} + r_{H_2} \tag{3.89}$$

$$\rho_3 = r_{SiO} + r_H \tag{3.90}$$

$$\rho_4 = r_{SiO} + r_{H_2} \tag{3.91}$$

$$\rho_5 = r_H + r_H \tag{3.92}$$

E_{Si} and E_{SiO} are activation energies required for the reactions between the interface traps and molecular hydrogen.

The consumptive variation of this model consists of reactions given below:

$$Si\bullet + H \xrightarrow{k_1} SiH \tag{3.93}$$

$$Si\bullet + H_2 \xrightarrow{k_2} SiH + H \tag{3.94}$$

$$SiO + H \xrightarrow{k_3} SiOH \tag{3.95}$$

$$SiO + H_2 \xrightarrow{k_4} SiOH + H \tag{3.96}$$

$$H + H \xrightarrow{k_5} H_2 \tag{3.97}$$

and the corresponding differential equations are

$$\frac{d}{dt}[Si\bullet] = -k_1\cdot[Si\bullet]\cdot[H] - k_2\cdot[Si\bullet]\cdot[H_2] \tag{3.98}$$

$$\frac{d}{dt}[SiO] = -k_3\cdot[SiO]\cdot[H] - k_4\cdot[SiO]\cdot[H_2] \tag{3.99}$$

$$\frac{d}{dt}[H] = -k_1\cdot[Si\bullet]\cdot[H] + k_2\cdot[Si\bullet]\cdot[H_2] - k_3\cdot[SiO]\cdot[H] + k_4\cdot[SiO]\cdot[H_2] - 2\cdot k_5\cdot[H]^2 \tag{3.100}$$

$$\frac{d}{dt}[H_2] = -k_2\cdot[Si\bullet]\cdot H_2] - k_4\cdot[SiO]\cdot[H_2] + k_5\cdot[H]^2 \tag{3.101}$$

where k_1, k_2, k_3, k_4 and k_5 are the same as those given in equations (3.83) to (3.87).

For both the non-consumptive and the consumptive cases, one unknown parameter is the activation energy for the reaction between SiO defects and hydrogen molecules, E_{SiO}. This parameter varies with E_{Si} and the concentration of SiO defects at the interface.

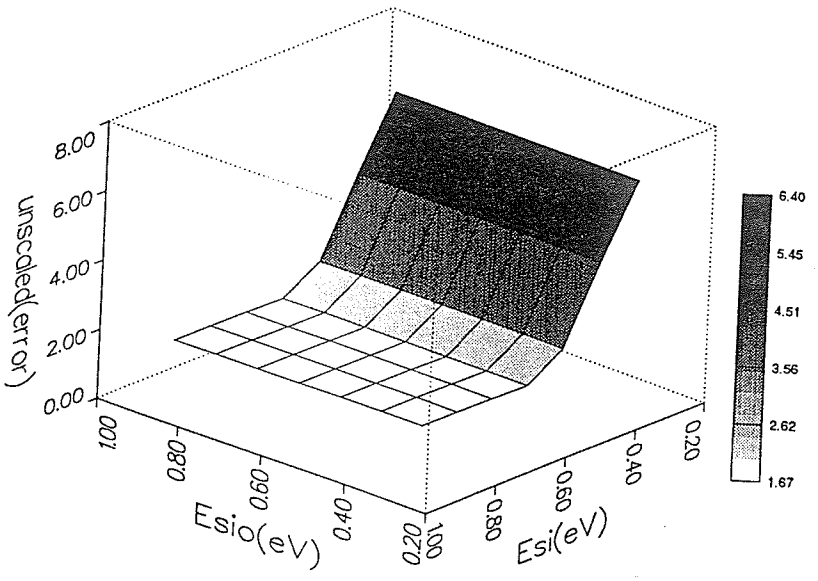

Figure 3.16: Computed value of the error term as a function of the silicon dangling bond capture cross section radius and the activation energy E_{SiO}

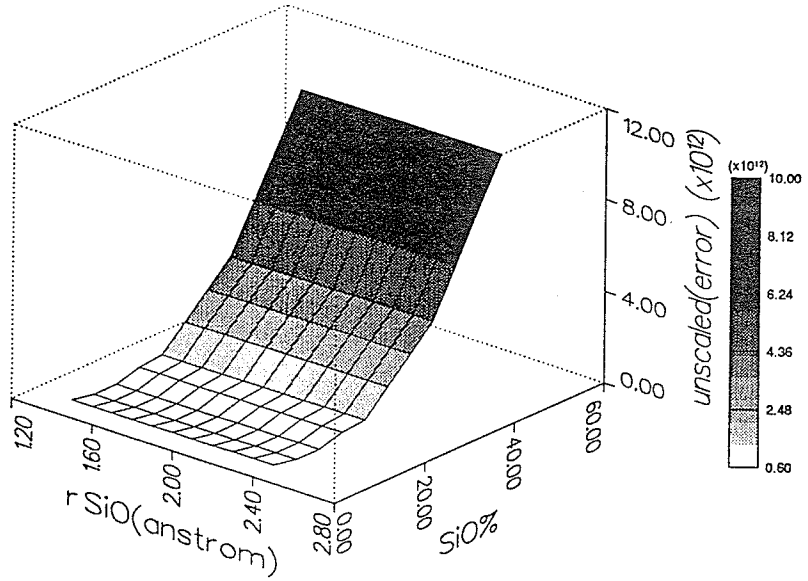

Figure 3.17: Computed value of the error term as a function of the SiO defect capture cross section radius and the SiO/Si• ratio

Figure 3.16 and 3.17 show that the value of the error term remains constant within the predicted range of E_{SiO}. This could be due to the fact that the amount of SiO defects is less than 10 percent of the total amount of interface traps. In addition to that, the reaction between SiO and H_2 is insignificant as compared to the reaction between SiO and H.

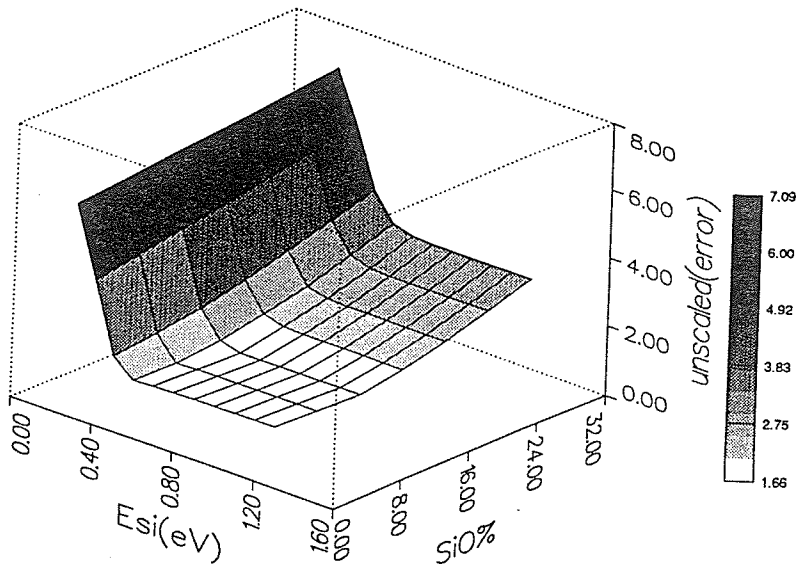

Figure 3.18: Computed value of the error term as a function of the activation energy E_{Si} and the SiO/Si• ratio

Figure 3.18 shows that the value of the error term increases very rapidly for E_{Si} less than 0.4eV indicating the importance of the role played by the activation energy.

One last simulation computation has performed with all the unknown parameters as variables. The results shows that the least value of the error term occurs when the parameters are given in Table 3.2.

Table 3.2: Values of the unknown parameters for the best fit to the experimental data

r_{Si}	1.6Å
E_{Si}	0.6eV
SiO%	5%
r_{SiO}	1.5-2.5Å
E_{SiO}	0.3-1.3eV

All these data are within realistic ranges and they agree well with theoretical predictions. Although the minimum value of the error term for the multi-reaction model is not significantly lower than the value of the error term for the two reaction model, it can explain the annealing phenomena better physically than the two reaction model. We can therefore conclude that the new multi-reaction model which includes the reaction of hydrogen molecules with silicon dangling bonds and SiO defects is a more complete model for describing the annealing processes.

CHAPTER 4

EFFECTS OF THE PLASMA TREATMENT OF SUBSTRATE SURFACES ON THE PERFORMANCE OF MOS DEVICES

4.1 Basic Principle of the Microwave PECVD Technique

Plasma, the fourth state of matters, is a mixture of ions, electrons and neutral atoms. The electrons in the microwave plasma are at very high energy states which are sustained by the energy supplied by electromagnetic radiation at a microwave frequency of 2.45 GHz. The electron temperature may reach 10^4K to 10^5K while the gas temperature may remain at 300K. This is due to the non-equilibrium between the gas molecules and the electrons. Inside the plasma, certain reactions can be carried out at relatively low gas temperatures which may, otherwise, need a much higher gas temperature to produce under normal conditions. This is because most of the energy required by the reactions in the plasma is provided by the electrons which are excited to very high energy states.

Chemical vapor deposition (CVD) of the SiO_2 can be done by mixing silane gas (SiH_4) and oxygen (O_2) at room temperature and atmospheric pressure to produce a spontaneous combustion. The SiO_2 formed this way is a white powdery deposit of colloidal silica that is useless in semiconductor technology. To produce high quality SiO_2 by a CVD process, the reaction between SiH_4 and O_2 has to be controlled. This can be done by diluting the SiH_4 in an inert gas such as helium or argon and allowing this gas mixture to react with O_2 at a pressure below 1 Torr. The reaction normally occurs at

temperatures in the range of 700°C to 900°C which exceed the limit for low temperatures processing. With the aid of a plasma, a gas temperature between 200°C and 500°C is sufficient for this reaction. This is the major reason that the plasma provides an important means for low temperature processing. The reaction between SiH_4 and O_2 can be described by

$$SiH_4 + O_2 \rightarrow SiO_2\ _{(solid)} + 2H_2 \qquad (4.1)$$

for the reaction under normal conditions at 700°C to 900°C, and by

$$O_2 \rightarrow 2O^* \qquad (4.2)$$

$$SiH_4 \rightarrow Si^* + 2H_2 \qquad (4.3)$$

$$Si^* + 2O^* \rightarrow SiO_2\ _{(molecule)} \qquad (4.4)$$

for the reaction enhanced by plasma at 200°C - 500°C.

The conventional thermal oxidation process is shown in Figure 4.1. In this process, oxygen molecules from the gas ambient diffuse through the oxide layer to the Si-SiO_2 interface and react with the silicon atoms there to form SiO_2. Silicon atoms are consumed at the interface but supplied from the silicon substrate.

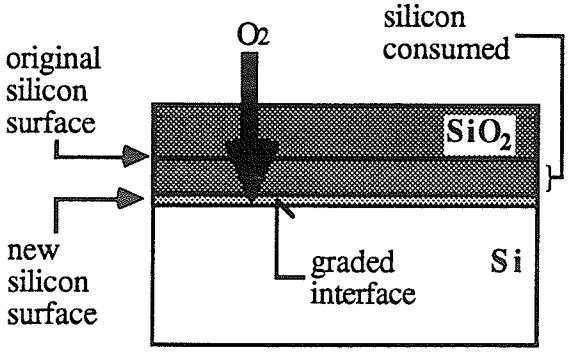

Figure 4.1: Schematic diagram showing the thermal oxidation process for the fabrication of SiO_2 films.

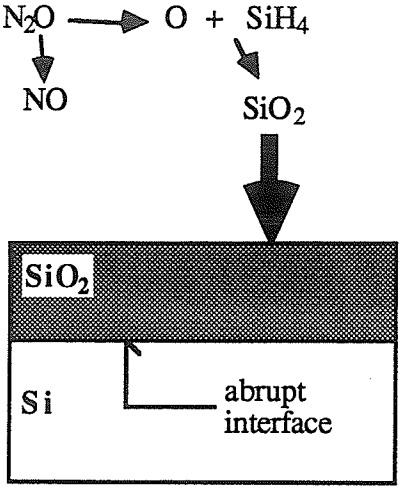

Figure 4.2: Schematic diagram showing the PECVD process for the fabrication of SiO_2 films.

In the PECVD process, silicon atoms are supplied from the silane gas. The silane reacts with the activated oxygen atoms or ions, that are formed due to the dissociation of N_2O gas in plasma, to form SiO_2 and H_2O. Silicon dioxide is then deposited layer by layer onto the silicon substrate and the water vapor is pumped out of the system. This process is illustrated in Figure 4.2.

N_2O molecules are dissociated by the microwave radiation into a variety of ions, atoms and electrons such as NO, NO+, O*, O+, and e-. The activated O* atoms and O+ ions are highly reactive and these species are essential to the reaction with silane to produce silicon dioxide molecules. The dissociation of N_2O and the reactions between the activated NO+, O* and O+ can be described by the following chemical reaction processes.

Dissociation of N_2O

$$N_2O \rightarrow NO + O^* \tag{4.5}$$

$$N_2O \rightarrow NO^+ + O^* + e^- \tag{4.6}$$

$$N_2O \rightarrow NO + O^+ + e^- \tag{4.7}$$

$$N_2O \rightarrow NO^+ + O^+ + e^- \tag{4.8}$$

Reaction with silane

$$SiH_4 + O^+ + O^* + e^- \rightarrow SiO_2 + 2H_2 \tag{4.9}$$

$$SiH_4 + NO^+ + O^* + e^- \rightarrow SiO_2 + NH_3OH \tag{4.10}$$

The PECVD process can be used not only for the deposition of SiO_2 films but also for Si_3N_4 films that are also vital to the performance of high quality VLSIs. One major barrier preventing the PECVD oxide to be used as the gate oxide is its high concentration of interface defects. Several investigators have reported that the interface characteristics can be improved by reducing the surface contaminants [8,39,40] or by altering the interface structures by particle bombardments [41,42].

The ECR microwave system used to produce the SiO_2 thin films was developed and built in the Materials and Devices Research Laboratory at the University of Manitoba [43]. This system has a short circuit or matched waveguide chamber to allow maximum power transfer from the source to the plasma. Two external coils are mounted around the waveguide chamber to provide an axial magnetic field to confine the plasma as well to produce an electron cyclotron resonance (ECR) condition. The system is schematically shown in Figure 4.3.

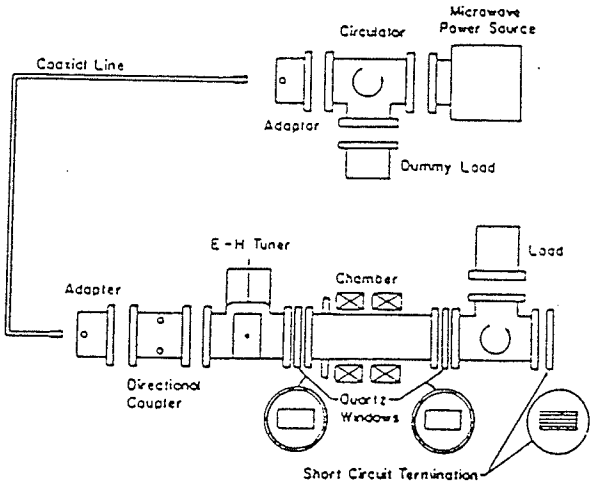

Figure 4.3: ECR microwave plasma system

4.2 N_2O Plasma Treatment

The presence of nitrogen at the Si-SiO_2 interface may improve the interface properties [44,45,46]. Nitrogen can be introduced to the interface by (1) nitrification of SiO_2 films in a nitrogen containing ambient, for examples, a mixture of hydrogen and nitrogen, NH_3, or (2) oxidation of silicon substrate in N_2O. Ting et al [47] have reported that the interface trap density of the oxide films grown in N_2O are lower than that of the oxide films grown in pure oxygen. It is generally believed that the nitrogen accumulated in the oxide bulk reacts with the SiO_2 to form SiO_xN_y [48]. The presence of SiO_xN_y at the

interface will release the interface strain due to the lattice mismatch between silicon and silicon dioxide, thus reducing the number of stress related defects. It has also been found that the PECVD oxide films grown by using SiH_4 and O_2 have a higher concentration of defects than those grown by using SiH_4 and N_2O [49]. This could be due to the reaction between SiH_4 and N_2O which may produce a better quality oxide, or due to a small amount of nitrogen incorporated into the oxide to form oxynitrates. However, the nitrogen concentration is below the detection limit of the FTIR, and no conclusion can be made about the involvement of nitrogen. If it is not due to the nitrogen incorporation, then the reaction between SiH_4 and N_2O may not be a simple direct process.

One way to improve the interface characteristics is to treat the silicon substrate in an N_2O plasma prior to the deposition of SiO_2. We have studied the effects of such a plasma treatment of the substrate surface. The substrates used for this investigation were n-type, <100> oriented, 3 - 8 ohm-cm silicon wafers. The substrates were thoroughly cleaned using the method described in detail in Appendix A with the main aim of removing the native oxide and contaminants originally present on the silicon surface. The cleaned substrates were then loaded into the processing chamber and the whole system was pumped down immediately to a base pressure of about 10^{-6} Torr in order to reduce the chance of oxidation. It has been shown that the silicon substrate after being cleaned in a 1% HF dip and DI rinse at the last stage of the RCA cleaning process has only a few monolayers of oxide when exposed to normal air atmosphere for 30 minutes [50]. The grown oxide layer is thinner if the cleaning does not involve DI rinse, possibly because the oxidation rate of silicon in water is much higher than in air.

The substrate is then exposed to N_2O plasma of various pressures for thirty minutes with the substrate temperature heated to 300°C. Five samples in each pressure are

examined to reduce the experimental and random errors. After the plasma treatment, a 200Å PECVD SiO_2 films are deposited onto the substrates. The details of the deposition technique are described somewhere else [51]. A complete description of the treatments and deposition parameters is shown in appendix A. Electrodes of 0.04 cm radii are then deposited onto the oxide films and the back of the substrate to form MOS capacitors. Interface trap densities are then calculated from data of the high frequency and quasi-static frequency capacitance-voltage measurements. The details of this method are described in appendix B. The interface trap densities with different pressures of N_2O plasma treatment are shown in Figure 4.4.

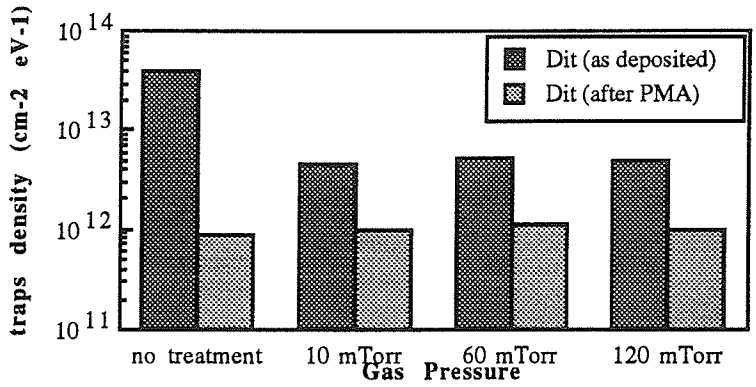

Figure 4.4: Interface trap density as a function of gas pressure of the N_2O plasma for devices as deposited and devices after PMA

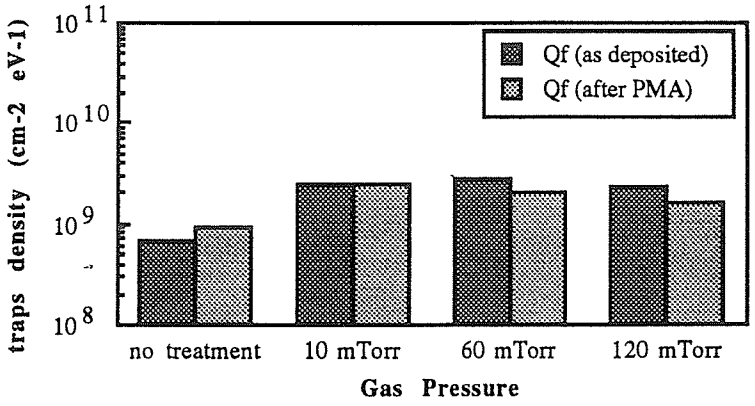

Figure 4.5: Oxide fixed charge as a function of gas pressure of the N_2O plasma for devices as deposited and devices after PMA

It can be seen from Figure 4.4 that the N_2O plasma treatment of the silicon substrate does reduce the interface trap density of the MOS devices as deposited but this effect is practically independent of the gas pressure. No noticeable change in D_{it} for the devices after post-metallization annealing (PMA) has been observed. Figure 4.5 shows that the N_2O plasma treatment of the silicon substrate causes an increase in Q_f, and this increase slightly reduces with increasing gas pressure. This phenomenon may be explained by the fact that nitrogen is a much weaker species than oxygen in its reaction with silicon. The reaction between nitrogen containing species and silicon can be expressed as

$$Si + aN \rightarrow SiN_a \tag{4.11}$$

$$Si + bNO \rightarrow SiN_cO_d \tag{4.12}$$

which are much slower than the reaction between oxygen and silicon which is expressed as

$$Si + O \rightarrow SiO \tag{4.13}$$

where variable a, b, c, and d are unknown constants since the structures of the end products are unknown. The slow reaction between nitrogen and silicon implies that the amount of nitrogen incorporated in the thermally grown SiO_2 films is much less as compared to oxygen. Furthermore, the silicon substrate is subject to a similar kind of treatment during film deposition because the substrate is exposed to N_2O plasma. Since the deposition parameters for all samples are the same, the effects of gas pressure for the N_2O plasma treatment may be covered up by the later plasma exposure. However, the decrease of the D_{it} is probably due to the formation of a SiO_xN_y layer on the silicon surface after the N_2O plasma treatment.

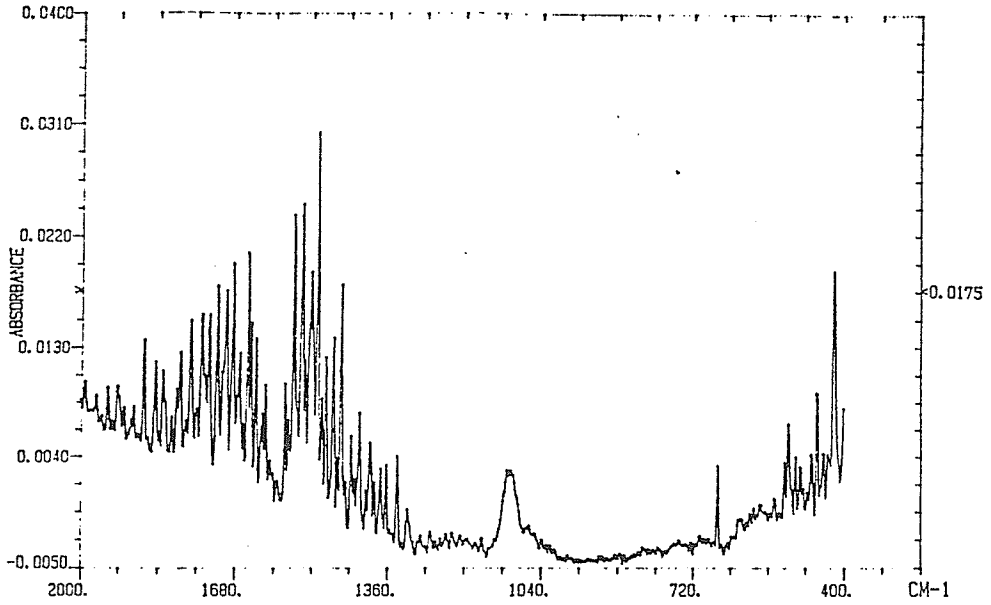

Figure 4.6: Absorption spectrum of the film produced after N_2O plasma treatment

After the N_2O plasma treatment, the substrate prior to the deposition of PECVD oxide film was immediately measured by FTIR spectroscopy. The reference substrate for this FTIR measurement was cleaned using the same method described above. Five hundred scans were done on both the reference without N_2O plasma treatment and the substrate after N_2O plasma treatment in order to reduce the noise to an acceptable level. Figure 4.6 shows clearly that there is a peak at about 1080 cm^{-1} corresponding to the absorption of SiO_2. If there is any nitrogen incorporated into the oxide film chemically, the absorption peak will shift to a lower wavenumber position.There is no noticeable shift of the SiO_2 peak in Figure 4.6 indicating that the amount of nitrogen incorporated in this film is small. The N_2O plasma treatment processes is shown schematically in Figure 4.7.

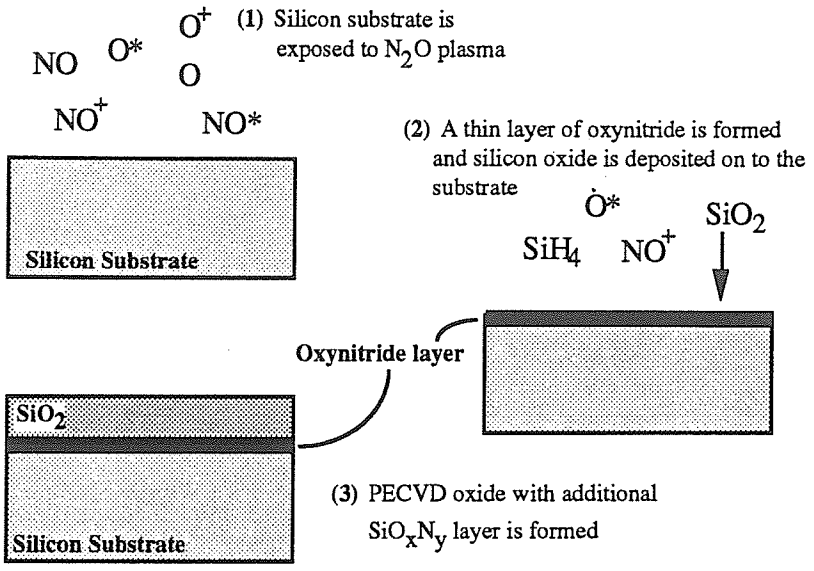

Figure 4.7: N_2O plasma treatment process

4.3 Nitrogen Plasma Treatment

In the previous section, we have mentioned that the N_2O plasma treatment reduces the interface trap density by a small amount. However, the role of the nitrogen played in the N_2O plasma treatment has not yet been determined. Therefore, we study the effects of nitrogen plasma treatment.

The same method as described in section 4.2 and Appendix A was used to clean the substrates. After cleaning, the substrates were treated in N_2 plasma for thirty minutes at gas pressures of 10 mTorr, 60 mTorr and 120 mTorr. The SiO_2 films were deposited immediately after the treatment. The whole experimental procedure was similar to that described previously. Figure 4.8 shows that the interface trap density after N_2 plasma treatment is almost one order lower than the untreated samples. The sample treated at a pressure of 60 mTorr gives a lower trap density than the others. Figure 4.9 shows the

FTIR spectrum of the substrate after nitrogen plasma treatment. In this spectrum there is a peak at 960cm^{-1} which corresponds to the absorption of SiN bonds.

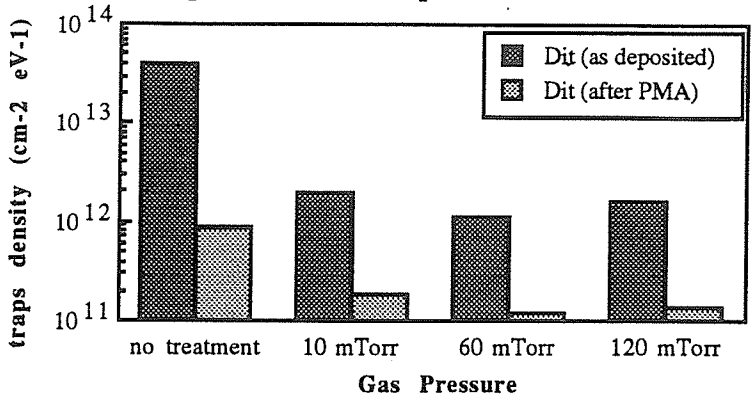

Figure 4.8: Interface trap density as a function of gas pressure of the N_2 plasma for the devices as deposited and the devices after PMA

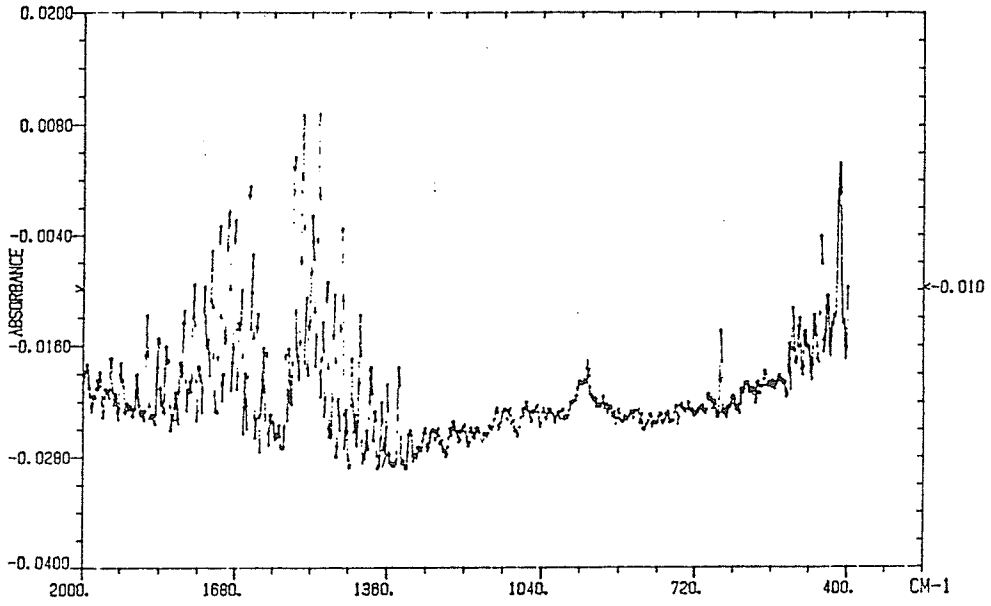

Figure 4.9: FTIR absorbance spectrum of the substrate after nitrogen plasma treatment

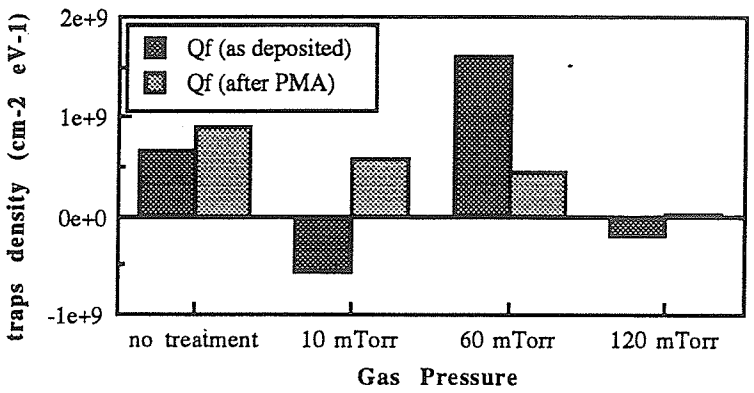

Figure 4.10: Oxide fixed charge density as a function of gas pressure of the N_2 plasma for the devices as deposited and the devices after PMA

The oxide fixed charge density as a function of gas pressure of the N_2 plasma is shown in Figure 4.10. It is interesting to note that the effect of the N_2 plasma treatment depends strongly on the gas pressure. For gas pressure of 10 mTorr and 120 mTorr, the oxide fixed charge becomes negative. However, the negative oxide fixed charge changes back to a positive charge after the samples being subjected to PMA in a forming gas at 400°C for 30 minutes. The appearance of negative oxide fixed charge is not surprising because it has been found that nitrification of silicon oxide would produce a negative shift in the flat band voltage [52]. This negative shift of the high frequency C-V curve increases as the nitrification time increases, but this shift may turn to the positive direction as the nitrification time exceeds a certain threshold [53]. The amount of negative shift of the flat band voltage is probably dependent on the amount of nitrogen present near the interface. Negative shift occurs when nitrogen atoms accumulate to a certain level and create sufficient electron traps following the reaction

$$\text{Si-O-Si} + \text{N} \rightarrow \text{SiO}\bullet + \text{SiN}\bullet \qquad (4.14)$$

It has to be noted that the actual structure of the traps is not known. However further nitrification will increase the amount of nitrogen at the interface and a more stable form of oxynitrates may be formed following the reaction

$$SiO\bullet + SiN\bullet + N \rightarrow SiO_xN_y \quad (4.15)$$

It is found that thin oxides have a much shorter turn around time for the flat band shift than thicker oxides. It is because time required for the nitrogen to diffuse to the interface is much shorter for thinner oxides. It is also found that the nitrification rate is higher at 60 mTorr than at other pressures. This could be due to the fact that at this particular pressure the amount of active species of nitrogen or oxygen inside the plasma is higher. That the glow of the plasma is more intense at this particular pressure is in support of this suggestion. This is also in agreement with the FTIR absorption spectrum. The nitrate layer is thicker after the 60 mTorr plasma treatment than that after 10 mTorr or 120 mTorr plasma treatments. When a thin nitrate layer is exposed to a highly reactive N_2O plasma, the active oxygen species will react with the silicon nitrate to form oxynitrates. For the samples having a thicker nitrate layer, more nitrogen is required for the formation of a more stable form of SiO_xN_y. However, for the samples having a thinner nitrates layer, the presence of nitrogen is insufficient for the formation of a stable form of SiO_xN_y, and then traps such as $SiO\bullet$ and $SiN\bullet$ are formed.

After annealing in forming gas, these traps are probably passivated by hydrogen and become inactive. Therefore, the flat band voltage shifts back to the positive side. The passivation of $SiO\bullet$ traps by hydrogen is highly probable based on the analysis given in chapter 3. The existence of $SiN\bullet$ as traps at the interface is still a question. However, there is always possibility that the presence of nitrogen at the interface promotes the formation of $SiO\bullet$ and SiO_xN_y and suppresses the formation of $SiN\bullet$. Further nitrification may completely eliminate the formation $SiO\bullet$ and produce more SiO_xN_y. The actual mechanism is not known at this point.

4.4 Oxygen Plasma Treatment

The presence of nitrogen at the Si-SiO_2 interface could indeed reduce the interface trap density and the oxide fixed charge density. One problem created by nitrogen plasma treatments is the formation of nitrification related defects such as SiO• or SiN•. This problem also occurs in films deposited with SiH_4 and N_2O because of the existence of nitrogen species inside the plasma. Deposition with O_2 may get rid of these problem but the electrical characteristics of the films deposited with O_2 are not as good as those deposited with N_2O.

One way to eliminate this nitrification related problem is to create a thin pure oxide layer before the deposition of SiO_2 with N_2O. This oxide layer has to be grown *in-situ* and grown with pure oxygen in order for it to be free of atmospheric contaminants and nitrogen. Since the oxide layer grown is very thin, it can be done at low temperatures within the temperature range for the PECVD process. The oxidation is produced in an oxygen plasma instead of oxygen gas for two reasons. One is the oxidation rate inside a plasma is higher than in oxygen gas, thus reducing the oxidation time, and the other is the oxygen plasma can remove organic contaminants from the substrate surface left behind by plastic wares used in the fabrication process, which the oxygen gas cannot. The high energy species from the plasma can disintegrate the carbon chains relatively easily and form volatile products following the reaction

$$\begin{array}{l} \quad H \quad H \\ \quad | \quad | \\ H-C-C-+O^* \rightarrow CO_2 + H_2O \\ \quad | \quad | \\ \quad H \quad H \end{array} \qquad (4.16)$$

The substrates after being cleaned using the method described in section 4.2 were treated in an oxygen plasma at various pressures prior to the deposition of the SiO_2 films. The results are given in Fig. 4.11 and 4.12.

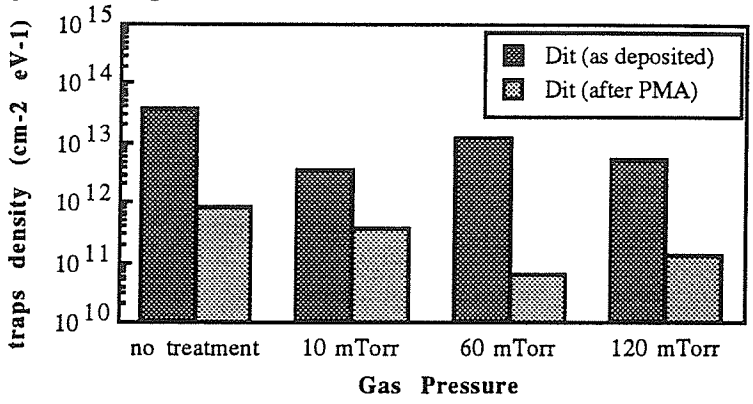

Figure 4.11: Interface trap density as a function of gas pressure of O_2 plasma for the devices as deposited and the devices after PMA

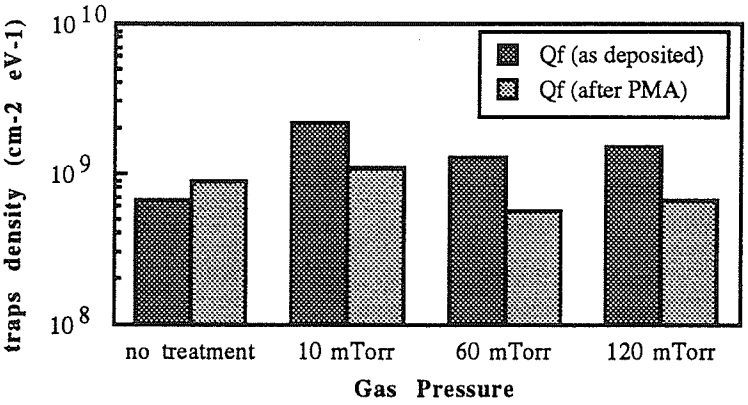

Figure 4.12: Oxide fixed charge density as a function of gas pressure of O_2 plasma for the devices as deposited and the devices after PMA

The samples treated in an oxygen plasma have a lower interface trap density and a lower oxide fixed charge density than those without treatment after annealing in forming gas. Again the lowest interface trap density and oxide fixed charge density occur at the gas pressure of 60 mTorr, in a similar manner for the N_2 plasma treatment. The effectiveness of the treatments depends on the amount of activated species present inside the plasma. It is found that the plasma glow is also brightest at this pressure indicating that a high

concentration of activated species inside the plasma occurs at this pressure. The FTIR absorption spectrums give further support of this finding. It is also found that the silicon oxide layer produced by the plasma at 60 mTorr is thicker as compared to those produced at other pressures. Therefore, it can be concluded that the oxide growth rate increases with increasing concentration of the activated species as expected. The thicker the oxide film grown by pure oxygen plasma, the better is its interface properties because the thicker oxide film has a better resistance to the nitrification of the oxide near the interface.

It should be noted that the interface trap density is higher for the samples treated by oxygen plasma than by N_2O or N_2 plasma before PMA in the forming gas. This means that the oxygen plasma treatment can reduce the amount of deep interface traps that cannot be passivated by PMA in the forming gas but it also create other kinds of traps which can be passivated by PMA. This explains why the samples have a higher interface trap density as deposited but have a lower trap density after annealing as compared to the samples with other treatments. This phenomenon is similar to that with rf argon plasma treatments. Oxygen plasma treatment can reduce the concentration of some kinds of traps that cannot be annealed out by forming gas annealing, but leave behind other kinds of traps that can be annealed out by forming gas annealing [42].

The increase in interface trap density after oxygen plasma treatment without PMA could be due to the bombardment of high energy ions or vacuum UV radiation or both. Since the oxide layers grown by oxygen plasma are only a few to ten monolayer thick, it is very susceptible to this kind of bombardments. That the plasma grown oxides cannot be very thick is mainly due to the low growing temperatures. The plasma can accelerate the growth of the first few monolayers of the oxide. Once the oxide reaches a certain thickness, the plasma cannot act effectively because the activated species will lose all their

energy to the SiO_2 layer before they can reach the silicon and react with it. The only process left is the thermal diffusion of oxygen species. At 300°C, the diffusivity of oxygen is relatively low and therefore the growth rate is very slow. At the same time, additional traps could be created in the following manner

$$\text{Si-O-Si} \xrightarrow{e^- \text{ or UV radiation}} \text{Si-O}\bullet + \text{Si}\bullet \tag{4.17}$$

The $SiO\bullet$ structure can act as an electron trap due to the high electron affinity of oxygen.

$$\text{Si-O}\bullet + e^- \rightarrow \text{SiO}:^- \tag{4.18}$$

The $Si\bullet$ structure can also act as a hole trap due to the relative low electron affinity of silicon.

$$\text{Si}\bullet \rightarrow \text{Si}^+ + e^- \tag{4.19}$$

By annealing in forming gas where hydrogen gas is present, these traps can be passivated by either

$$\text{SiO}\bullet + \text{Si}\bullet \rightarrow \text{Si-O-Si} \tag{4.20}$$

or they could react with hydrogen to form electrical inactive species.

$$\text{Si}\bullet + \text{H} \rightarrow \text{SiH} \tag{4.21}$$

$$\text{SiO}\bullet + \text{H} \rightarrow \text{SiOH} \tag{4.22}$$

Experimental results of the N_2O, N_2 and O_2 plasma treatments are summarized in Table 4.1. All the surface treatments are performed at 60 mTorr and followed by PECVD of SiO_2 films using SiH_4 and N_2O. Although N_2O and N_2 plasma treatments shows that nitrogen incorporation at the interface can reduce the interface defect density, a pure oxide layer formed by O_2 plasma treatment has the lowest interface trap density, the PECVD SiO_2 films fabricated using SiH_4 and N_2O have better interface and bulk properties than those

using SiH_4 and O_2. This implies that the dependence of D_{it} and Q_f are not only related to the chemical composition but also the reaction processes during deposition.

Table 4.1: Interface trap density of oxide films with various plasma treatments after PMA

	D_{it} ($cm^{-2}eV^{-1}$)
deposited by SiH_4 and O_2	$>10^{12}$
deposited by SiH_4 and N_2O	$8.7x10^{11}$
N_2O plasma treatment	$7.6x10^{11}$
N_2 plasma treatment	$1.5x10^{11}$
O plasma treatment	$7.5x10^{10}$

4.5 Hydrogen Plasma Treatment

Several investigators [54,55,56] have suggested that hydrogen plasma can be used for removing the native oxide and other contaminants from the silicon substrate. Hydrogen plasma can react with very stable materials such as SiO_2 and form volatile products because of its high reactivity. The reaction with SiO_2 can produce SiH_4 and H_2O.

$$SiO_2 + 8H^* \rightarrow SiH_4 + 2H_2O \qquad (4.23)$$

For hydrogen plasma treatment, the silicon substrates were loaded into the processing chamber without being subject to any cleaning process. They were treated in an hydrogen plasma for various lengths of time prior to the deposition of a 200Å SiO_2 films. The results are shown in Fig. 4.13.

The hydrogen plasma treatment has a negative effect on the interface trap density. A few mechanisms are responsible for this degradation. Two of them are the ion bombardment and the vacuum UV radiation. The third one is the native oxides which cannot be totally removed from the silicon substrate in this case. The FTIR spectrum shows no obvious difference between the native oxides before and after hydrogen plasma

treatments, possibly due to only a small structural alteration done by the plasma. It is likely that this small change in structure does not show up physically but it gives a more significant effect electrically.

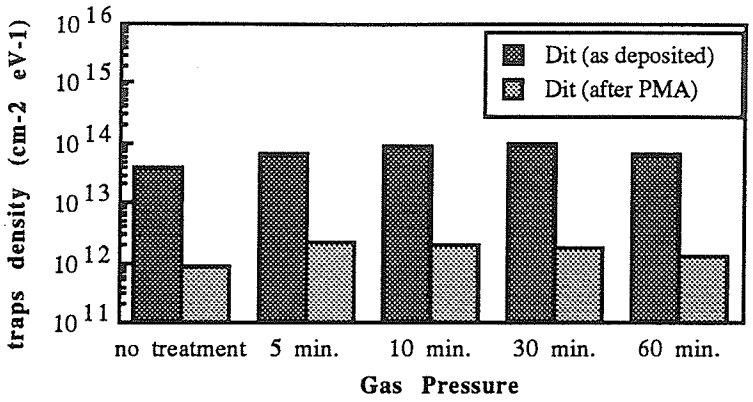

Figure 4.13: Interface trap density as a function of gas pressure of the H_2 plasma for the devices as deposited and the devices after PMA

Insufficient power input from the microwave power supply may also result in a lower ionization and a lower energy of activated species. The consequence is that the reaction shown in equation 4.18 cannot be completed, and cause the formation of a hydrogenated layer of native oxide. Defects can be generated in the following manner.

$$\text{Si-O-Si} + \text{H} \rightarrow \text{SiOH} + \text{Si}\bullet \qquad (4.24)$$

$$\text{Si-O-Si} + \text{H} \rightarrow \text{SiH} + \text{SiO}\bullet \qquad (4.25)$$

We have performed an experiment with the substrates cleaned before H_2 treatment. Silicon substrates were cleaned as described in previous sections to remove the native oxides and possible contaminants, and then treated in N_2O plasma for 30 minutes to produce an oxide layer which acts as the native oxide. The treatment in hydrogen plasma for 30 minutes is to simulate the hydrogen plasma treatment of the native oxides. With such treatment, the interface trap densities for both cases are given in Table 4.2.

Table 4.2: Interface trap density of the films with native oxide and N_2O plasma oxide after hydrogen plasma treatment and PMA

	D_{it} ($cm^{-2}eV^{-1}$)
native oxide	$1.5x10^{12}$
N_2O plasma oxide	$1.4x10^{12}$

The increases in the interface trap density for the samples cleaned and the plasma treated samples as well as the samples with the real native oxide prior to the H_2 treatment is due to the incomplete removal of the native oxide which has a have negative effect on the interface properties. These results seem to conflict those presented earlier [38] for that silicon substrates were cleaned and treated by N_2O plasma and then followed by hydrogen plasma treatment. The results from that experiment show a positive effect in reducing the interface trap density. The big difference is mainly due to the presence of the SSEC device between the plasma and the silicon substrate in the former experiment. These results are summarized in Table 4.3.

Table 4.3: Interface trap density of the films with N_2O plasma treatment followed by H_2 plasma treatment

	D_{it} ($cm^{-2}eV^{-1}$)
without SSEC	$1.5x10^{12}$
with SSEC	$3.2x10^{10}$

The use of the SSEC device to filter out all the high energy hydrogen species and the vacuum UV radiation which are responsible for creating the defects. Low energy hydrogen species passing through the SSEC device are responsible for the passivation of the interface traps without creating more defects. This is because the low energy species are active enough to passivate the traps but they do not have enough energy to cause damage in the SiO_2 structure.

CHAPTER 5

CONCLUSIONS

On the basis of the results from the numerical analysis and the experiments given above, the following conclusions are drawn:

(1) The interface trap density of the Si-SiO_2 system without active metal electrodes can be reduced by thermal annealing in an ambient containing hydrogen gas. This indicates that apart form atomic hydrogen, molecular hydrogen is also responsible for the annealing. Numerical analysis also show that molecular hydrogen is another species capable of passivating the interface traps.

(2) The interface trap generation model suggests that SiO is electrically active at the interface. The results of the numerical analysis support this suggestion and that about 5% of the interface traps are due to SiO defects and the rest are due to silicon dangling bonds.

(3) The multi-reaction model taking into account the SiO defects and the reactions between the interface traps and the hydrogen molecules explains well the reduction of interface traps of the Si-SiO_2 system without gate electrode by annealing in a medium containing hydrogen gas.

(4) The capture cross section of the silicon dangling bonds is about 1.6Å and the activation energy for the reaction between the hydrogen molecules and silicon dangling bonds is about 0.6eV based on the numerical analysis.

(5) The N_2O plasma treatment of the silicon substrate surface reduces slightly the D_{it} but introduce more Q_f. The nitrogen plasma treatment reduces the amount the D_{it} by one order, and it also introduces a negative shift of the flat band voltage which can be reversed by post-metallization annealing (PMA).

(6) The oxygen plasma treatment of the silicon substrate surface reduces the D_{it} to the order of 10^{10} cm^{-2} eV^{-1} which is comparable to the high quality thermal oxide. It is believed that a very thin high quality thermal oxide formed prior to the PECVD of the SiO_2 film is responsible for the improvement. This proves to be a very compromising technique for PECVD oxides.

(7) The hydrogen plasma treatment of the silicon substrate surface does not remove the native oxide entirely and leaves behind an oxide layer which has a higher defect concentration.

(8) The effectiveness of the plasma treatment depends on the concentration of the active species which in turn depends on the gas pressure. The optimum pressure for nitrous oxide, nitrogen and oxygen for the plasma treatment of the silicon substrate surface is about 60 mTorr.

REFERENCES

[1] S. T. Ang, J. J. Wortman, J. Electrochem. Soc., **133**, 2361 (1986)

[2] J. Batey, E. Tierney, J. Appl. Phys., **60**, 3136 (1986)

[3] G. G. Fountain, R. A. Rudder, S. V. Hattangady, and R. J. Markunas, J. Appl. Phys,**63**, (1988)

[4] T. T. Chau, S. R. Mejia, K. C. Kao, Electron. Lett., **25**, 1088 (1989)

[5] B. Robinson, T. N. Nguyen, and M. Copel, in *Deposition and Growth: Limits for Electronics*, Edited by G. W. Rubloff (Materials Research Society, Anaheim, CA, 1987), p. 112.

[6] T. T. Chau, S. R. Mejia, K. C. Kao, Mater. Res. Soc. Proc. 225 (Anaheim, CA, 1991)

[7] T. T. Chau, S. R. Mejia, K. C. Kao, J. Vac. Sci. Technol., **B9**, Jan/Feb, 50 (1991)

[8] T. Yasuda, Y. Ma, S. Habermehl, and G. Lucovsky, Appl. Phys. Lett., **60**, 434 (1992)

[9] M. Delfino, S. Salimian, D. Hodul, A. Ellingboe, and W. Tsai, J. Appl. Phys, **71**, 1001 (1992)

[10] S. Kar, Solid State Electronics, **18**, 723 (1974)

[11] B. K. Ip, K. C. Kao, and D. J. Thomson, Solid States Electronics, **34**, 123 (1991)

[12] M. L. Reed, J. D. Plummer, J. Appl. Phys., **63**, 5776 (1988)

[13] K. L. Brower, Phys. Rev. B, **38**, 9657 (1988)

[14] B. E. Deal, J. Electrochem. Soc., **121**, 198C

[15] P. Balk, in *Proceeding of the Electrochemical Society Fall Meeting* (Electrochemical Society, Buffalo, NY, 1965), p. 29

[16] R. A. Clarke, R. L. Tapping, M. A. Hopper, and L. Young, J. Eletrochem. Soc., **122**, 1374 (1975)

[17] J. Blanc, C. J. Buiocchi, M. S. Abrahams, and W. E. Ham, Appl. Phys. Lett., **30**, 120 (1977)

[18] O. L. Krivanek, T. T. Sheng, and D. C. Tsui, Appl. Phys. Lett., **32**, 437 (1978)

[19] E. H. Nicollian and J. R. Brews, *MOS (Metal Oxide Semiconductor) Physics and Technology* (Wiley, New York, 1982), Chap. 6

[20] A. Ourmazd and Bevk, in *Material Research Society Symposium Proceedings*, **105**, p. 1 (1988)

[21] D. E. Aspnes and J. B. Theeten, J. Electrochem Soc., **127**, 1359 (1980)

[22] G. W. Rubloff, in *Material Research Society Symposium Proceedings*, **105**, p. 11 (1988)

[23] S. Kar and W. E. Dahlke, Solid States Electronics, **15**, 221 (1972)

[24] E. H. Nicollian and J. R. Brews, *MOS (Metal Oxide Semiconductor) Physics and Technology* (Wiley, New York, 1982), Chap. 10

[25] S. M. Sze, *Physics of Semiconductor Devices*, (Wiley, New York, 1981), Chap. 9

[26] C. M. Berglund and R. J. Powell, J. Appl. Phys., **42**, 573 (1971)

[27] D. J. DiMaria and D. W. Dong, J. Appl. Phys., **51**, 2722 (1980)

[28] S. K. Lai and D. R. Young, J. Appl. Phys., **52**, 6231 (1981)

[29] A. Goetzberger, V. Heine, and E. H. Nicollian, Appl. Phys. Lett., **12**, 95 (1968)

[30] T. Sakurai and T. Sugano, J. Appl. Phys., **52**, 2889 (1981)

[31] E. H. Nicollian and J. R. Brews, *MOS (Metal Oxide Semiconductor) Physics and Technology* (Wiley, New York, 1982), Chap. 16

[32] Y. Nishi, Jap. J. Appl. Phys., **10**, 51 (1971)

[33] E. H. Poindexter, E. R. Ahlstrom and P. J. Caplan, in *The Physics of SiO_2 and Its interfaces*, S. T. Pantelides, Ed., Pergamon, New York, Chap. 4

[34] B. J. Fishbein, J. T. Watt, and J. D. Plummer, J. Electrochem. Soc., **134**, 674 (1987)

[35] M. L. Reed, J. D. Plummer, IEEE Trans. Nuclear Sci., **NS-33**, 1198 (1986)

[36] C. Sah, J. Y. Sun, J. J. Tzou, J. Appl. Phys., **53**, 8886 (1982)

[37] N. M. Johnson, D. K. Biegelsen, M. D. Moyer, V. R. Deline, and C. A. Evans, Jr., Appl. Phys. Lett., **38**, 995 (1981)

[38] D. Y. Chung, *The Annealing Effects on the Properties of SiO2 Thin Films Fabricated by ECR Microwavw Process* (B. Sc. Thesis, University of Manitoba, (1991)

[39] W. Kern, J. Electrochem. Soc., **137**, 1887 (1990)

[40] S. Salimian and Delfino, J. Appl. Phys., **70**, 3970, (1991)

[41] J. Kassabov, E. Atanassova, and D. Dimitrov, Solid States Electronics, **31**, 147 (1988)

[42] J. Kassabov, E. Atanassova, D. Dimitrov, and E. Goranova, Microelectronics Journal, **18**, No. 5, 5 (1987)

[43] S. R. Mejia, *The Effects of Deposition Parameters on Hydrogenated Amorphous Silicon Films Fabricated by Microwave Glow Discharge Techniques* (M.Sc. Thesis, University of Manitoba, 1984)

[44] T. Ito and T. Nakamura, IEEE Trans. Electron. Devs., **ED-29**, 498 (1982)

[45] H. Hwang, W. Ting, B. Maiti, D. Kwong, and J. Lee, Appl. Phys. Lett., **57**, 1010 (1990)

[46] D. K. Shih and D. L. Kwong, Appl. Phys. Lett., **54**, 822 (1989)

[47] W. Ting, H. Hwang, J. Lee, and D. L. Kwong, Appl. Phys. Lett., **57**, 2808 (1990)

[48] R. P. Vasquez and A. Madhukar, Appl. Phys. Lett., **47**, 998, (1989)

[49] K. C. Kao, private communication.

[50] E. A. Taft, J. Electrochem. Soc., **135**, 1022 (1987)

[51] T. T. Chau, *title*, (M. Sc. Thesis, Universoty of Manotoba, 1988)

[52] K. P. Poenker, *Silicon Nitride and Silicon Dioxide Thin Insulating Films*, Proceeding of The Electrochem. Soc., **87-10**, p.115

[53] T. Ito, T. Nakamura, and H. Ishikawa, J. Electrochem. Soc., **129**, 184 (1982)

[54] M. Ishii, K. Nakashima, I. Tajima, and M. Yamamoto, Appl. Phys. Lett., **58**, 1378 (1991)

[55] T. Koui, I. Suemune, A. Kishimoto, K. Hamaoka, and M. Yamanishi, Jap. J. Appl. Phys., **30**, 3202 (1991)

[56] K. Nakashima, M. Ishii, I. Tajima, and M. Yamamoto, Appl. Phys. Lett., **58**, 2663 (1991)

APPENDIX A

SiO_2 DEPOSITION AND Si SURFACE TREATMENT PARAMETERS

The following parameters are common in all experiments except the cleaning procedures which are not used for the hydrogen plasma treatment experiments for samples with native oxides

Wafers n-type, <100> oriented, 2-4 Ω-cm, 3" in diameter

Cleaning Procedures

1. acetone rinse for 1 minute
2. deionized water rinse for 1 minute
3. methanol rinse for 1 minute
4. deionized water rinse for 1 minute
5. submersion in $NH_4OH : H_2O_2 : H_2O$ (5:1:1) at about 80°C for 10 minutes
6. deionized water rinse for 1 minute
7. 1% HF dip for 15 seconds
8. deionized water rinse for 1 minute
9. submersion in $HCl : H_2O_2 : H_2O$ (6:1:1) at about 80°C for 10 minutes
10. deionized water rinse for 1 minute
11. submersion in $HF : H_2O$ (1:100) for 15 to 30 seconds depending upon the time required for the complete removal of the oxide.

Samples Used in the Experiments Described in Chapter 3

Deposition Parameters

Time:	13 minutes
Temperature	300°C
Flow ($SiH_4 : N_2O$)	1 : 10 sccm
Power	4 Watts
Pressure	26.2 mTorr
DC Magnetic Current	23 Ampre

Samples Used in the Experiments in Chapter 4

Deposition Parameters

Time:	30 minutes
Temperature	300°C
Flow (SiH_4 : N_2O)	1 : 10 sccm
Power	1.8 - 2.2 Watts
Pressure	13.5 - 14.5 mTorr
DC Magnetic Current	23 Ampre

Plasma Parameters for Si Substrate Surface Treatment

gas type	pressure (mTorr)	gas flow (sccm)	power absorbed (W)	temperature (°C)	Si substrate surface treatment time (min)
N_2O	10	6.8	1.6	300	30
N_2O	60	2.5	4	300	30
N_2O	120	7.0	7	300	30
N_2	10	7.7	0.9	300	30
N_2	60	3.5	2.5	300	30
N_2	120	9.7	3.8	300	30
O_2	10	7.8	6.3	300	30
O_2	60	1.8	2.7	300	30
O_2	120	8.8	3.4	300	30
H_2	60	8.0	3.8	300	30

N_2O-H_2 Plasma Parameters

N_2O Plasma Treatment	same as N_2O plasma treatment at gas pressure of 60 mTorr
H_2 Plasma Treatment	same as H_2 plasma treatment but for samples with native oxides

APPENDIX B

CAPACITANCE-VOLTAGE (C-V) METHODS FOR THE DETERMINATION OF TRAPS DENSITIES

B.1 The High Frequency C-V and the Quasi Static (Low Frequency) C-V Method for the Determination of the Interface Trap Density

The high-low frequency C-V method has been commonly usedfor the determination of the interface trap density. This method is superior to the high frequency C-V method alone or the quasi static (low frequency) C-V method alone because it does not involve the computation of the theoretical C-V curves under trap free conditions. The high frequency C-V curves are usually measured at a frequency in the MHz range. At such a high frequency, the interface trapped charge cannot follow the small signal ac gate voltage, but follow the gate bias as the MOS capacitor is swept from the accumulation to the inversion mode. The capacitance per unit area measured at a high frequency (about 1MHz) can be written as

$$\frac{1}{C_{HF}} = \frac{1}{C_{OX}} + \frac{1}{C_j} \tag{B.1}$$

or

$$C_{HF} = \frac{C_{OX} + C_j}{C_{OX} \cdot C_j} \tag{B.2}$$

where C_{OX} is the oxide capacitance per unit area which is given by

$$C_{OX} = \varepsilon_{OX} / d \tag{B.3}$$

and C_j is the depletion region capacitance which is given by

$$C_j = \varepsilon_S / W \tag{B.4}$$

in which ε_{OX} and ε_S are, respectively, the permitivities of the oxide and the silicon semiconductor, d and W are, respectively, the oxide thickness and the depletion region depth in the silicon semiconductor.

For the measurement of the low frequency C-V curves, we should use a frequency of the order of 1 Hz for the small signal ac voltage so that the interface trapped charge can

follow the small signal ac voltage. However, it is much more convenient to measure the quasi static C-V curves by measuring the current, I, using a linear ramp voltage with the capacitance (C) calculated from the following relation

$$C = I(\frac{dV}{dt})^{-1} \tag{B.5}$$

Since I is a function of V, if the ramp rate is small, the C-V curve obtained by this method is equivalent to the low frequency C-V curve. The capacitance measured by this method can be written as

$$\frac{1}{C_{LF}} = \frac{1}{C_{OX}} + \frac{1}{C_j + C_{it}} \tag{B.6}$$

or

$$C_{it} = (\frac{1}{C_{LF}} - \frac{1}{C_{OX}})^{-1} - C_j \tag{B.7}$$

where C_{it} is the capacitance due to the presence of the interface trapped charge. Substituting (B.1) into (B.5), we have

$$C_{it} = (\frac{1}{C_{LF}} - \frac{1}{C_{OX}})^{-1} - (\frac{1}{C_{HF}} - \frac{1}{C_{OX}})^{-1} \tag{B.8}$$

C_{it} can be expressed as

$$C_{it} = \frac{dQ_{it}}{d\psi_S} = \frac{q \cdot dD_{it}}{d\psi_S} \tag{B.9}$$

where ψ_S is the surface potential. Thus the interface trap density can be expressed as

$$D_{it} = \frac{1}{q}[(\frac{1}{C_{LF}} - \frac{1}{C_{OX}})^{-1} - (\frac{1}{C_{HF}} - \frac{1}{C_{OX}})^{-1} \tag{B.10}$$

D_{it} is measured in the number of interface traps per $cm^{-2}eV^{-1}$. Normally D_{it} is a function of gate voltage (V_G). Since ψ_S is a function of V_G, so we can map D_{it} versus energy level in the silicon band gap. In general, we use the value of D_{it} at the energy level around the midgap to represent the normal value of D_{it}. The energy level of the traps relative to the energy level of the conduction band edge can be written as

$$\frac{E - E_C}{q} = \frac{E_g}{2q} + \psi_S - \psi_B \qquad (B.11)$$

in which, ψ_S is given by

$$\psi_S = \int_{V_{fb}}^{V_G} [1 - \frac{C_{LF}(V_G)}{C_{OX}}] \, dV_G \qquad (B.12)$$

where E_g is the width of the band gap of silicon and ψ_B is the difference between the Fermi level and the intrinsic Fermi level. A computer program is used to calculate D_{it} as a function of E_C - E.

The experimental arrangement for measuring the high frequency C-V curves is shown in Figure B.1 and that for measuring the quasi static C-V curves is shown in Fig. B.2.

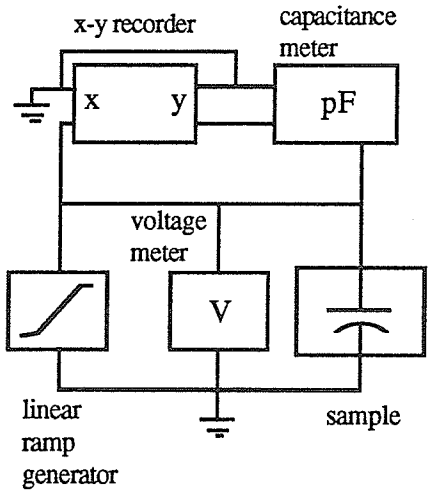

Figure B.1: Experimental arrangement for the measurements of the high frequency C-V curves

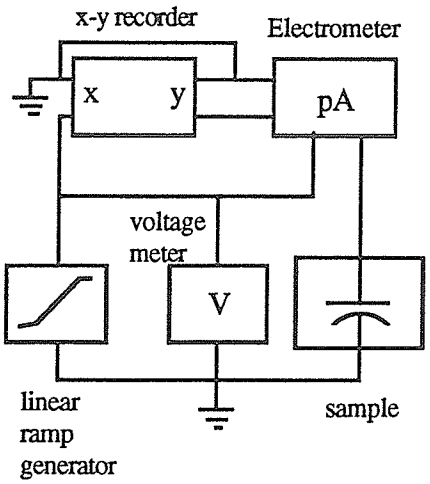

Figure B.2: Experimental arrangement for the measurements of the quasi static C-V characteristics

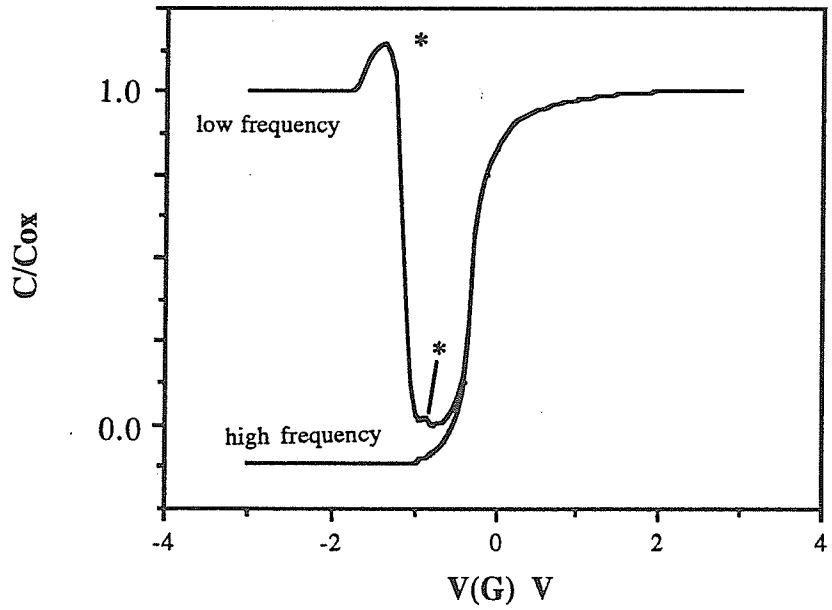

Figure B.3: The high frequency C-V curve and the quasi static C-V curve used for determining the interface trap density

The high frequency and the quasi static C-V curves of a typical MOS capacitor are shown in Figure B.3. From the C-V curves, it can be seen that the threshold voltage for strong inversion is about 1V. This value is acceptable for device applications. There is an elevation of the quasi static C-V curve at the position marked (*) which is normally not

found in thermal oxide devices. This may be due to a certain kind of traps with a limited band of energy levels present at the Si-SiO_2 interface. One possible cause is the abrupt interface where the dangling bonds reacts with water molecules resulting in the presence of OH groups there. Besides the presence of the OH groups, other impurities entering the silicon surface, which may not be removed by the normal cleaning procedure, may also be the candidate for this phenomenon. This kind of traps is not found in the thermal oxide. This may be due to the fact that these impurities may remain at the metal-oxide interface after the oxide has been grown. Since they are not present at the Si-SiO_2 interface, they do not contribute to the concentration of the interface traps. It is also known that the Si-SiO_2 interface for the PECVD SiO_2 films is simply the silicon surface, thus impurities can be easily trapped at the interface due to the high concentration of dangling bonds and act as interface traps.

B.2 Oxide Fixed Charge Measurements by the High Frequency C-V Method

Since the oxide fixed charge remains unchanged after a low temperature annealing, it can be isolated by annealing out the interface trapped charge and the oxide trapped charge. Moreover, the drift of the mobile ion charges at room temperature can be neglected due to their low mobility, therefore the values of the oxide fixed charge can be evaluated using only the high frequency C-V method.

One of the most important features of the high frequency C-V curve is that it can reveal the net charge present inside the oxide by a shift of the ideal curve under the charge free condition. Besides the net charge inside the oxide, the work function difference (ϕ_{MS}) between the silicon substrate and the metallic gate can also cause a shift of the high

frequency C-V curve. Typical shift of the high frequency C-V curves before and after annealing is shown in Figure B.4. The flat-band shift of the high frequency C-V curve is V_{fb} and it is due to the presence of oxide fixed charge and the work function difference.

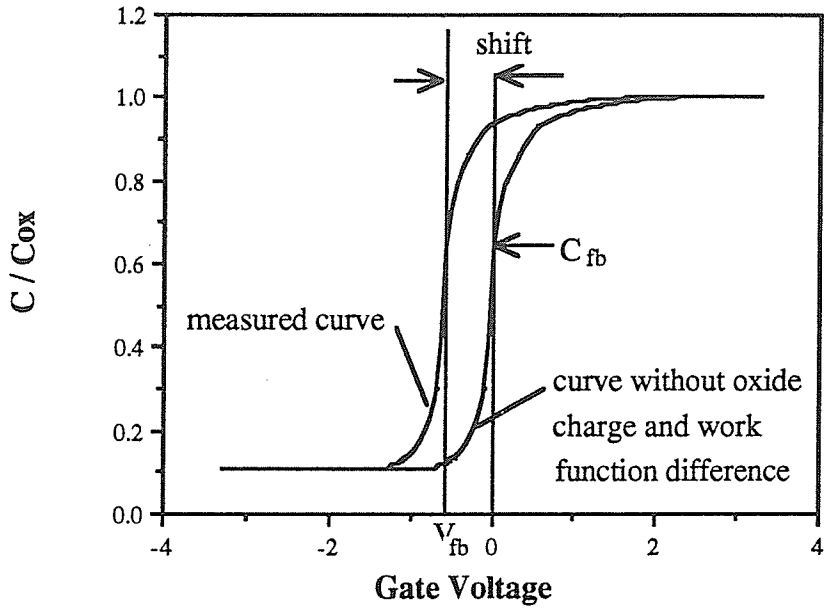

Figure B.4: Typical high frequency C-V curves with and without Q_f. The Flat band shift V_{fb} is equal $\phi_{MS} + \phi_f$

Thus the oxide fixed charge can be written as

$$Q_f = C_{OX} \cdot (V_{fb} - \phi_{MS}) \qquad \text{(B.13)}$$

where C_{OX} is the oxide capacitance per unit area which is given by

$$C_{OX} = \varepsilon_{OX}/d \qquad \text{(B.14)}$$

ε_{OX} and d are, respectively, the permittivity and the thickness of the oxide. V_{fb} is the flat band voltage which is the gate voltage required to make the energy band of the Si flat at the Si-SiO_2 interface, $\phi_{MS} = \phi_M - \phi_S$ is the difference between the work function of the metal ϕ_M and the work function of the silicon ϕ_S. Normally ϕ_M is constant but ϕ_S depends on the doping concentration of the silicon. The value of the oxide fixed charge density for the

thermal oxide depends strongly on the oxidation temperature but that for the PECVD oxide is practically independent of the deposition temperature.

APPENDIX C

COMPUTER PROGRAM FOR THE CALCULATION OF INTERFACE TRAP DENSITIES

The computer program accepts the input of the high frequency and the quasi-static capacitance-voltage curves and calculates the oxide thickness, dopant concentration, flat band voltage, metal-semiconductor workfunction difference and the interface trap densities at various energy levels. This program is written based on the Lightspeed Pascal version 1.11 and can be run on any Macintosh computer. It consists of six units. They are, respectively, the main program, the variables, the env, the newdata, the cdata and the I/O. A brief description and the flow chart for each unit are shown below and the program listing is followed.

main program

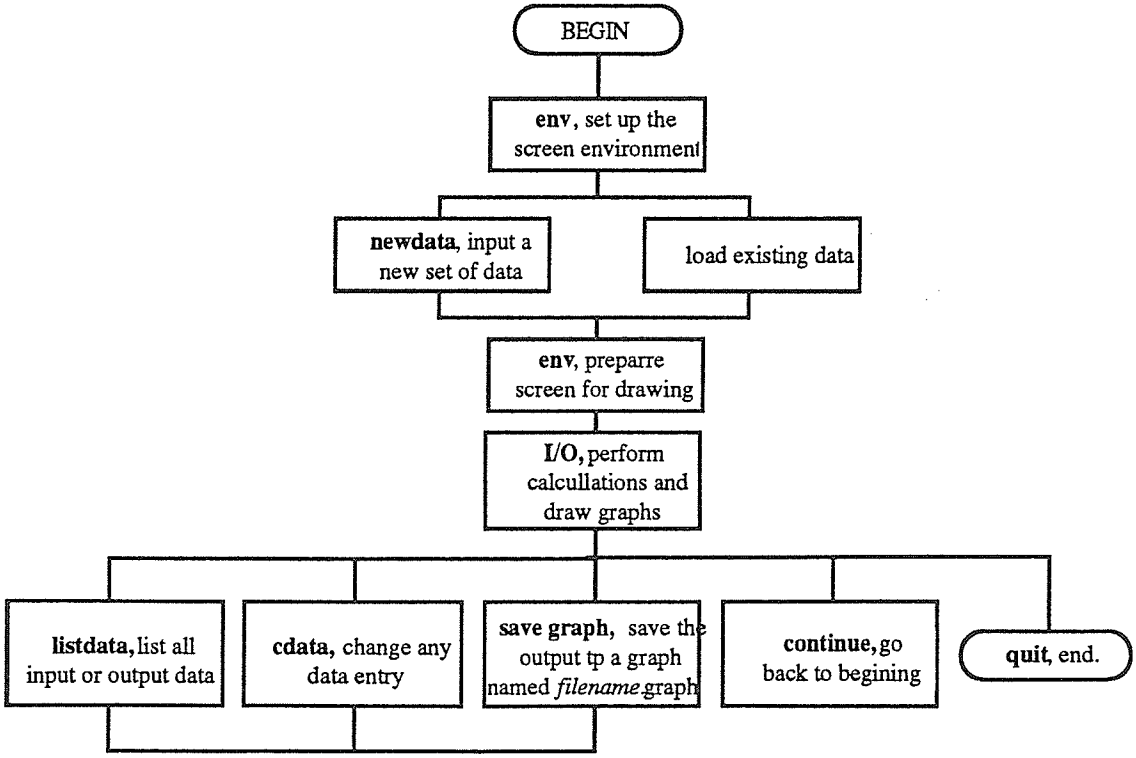

variables

This unit contains all the global variables used in the program.

env

This unit sets up the screen environment for outputs.

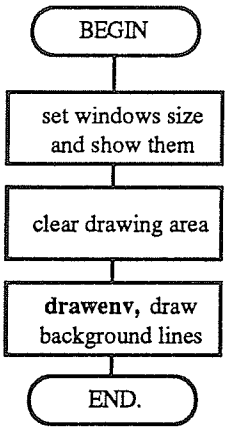

newdata

This unit takes all tje inputs and stores it in a file whose name is specifed by user.

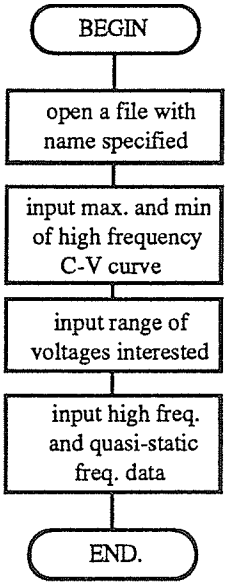

cdata

This unit is for changing any data entered.

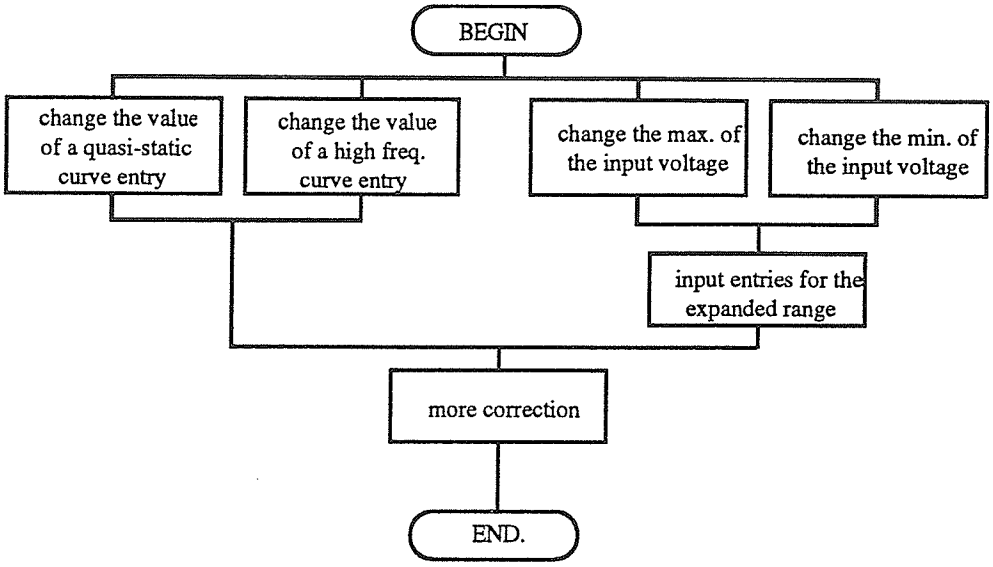

listdata

This procedure is for listing all the input data ot all the calculated data.

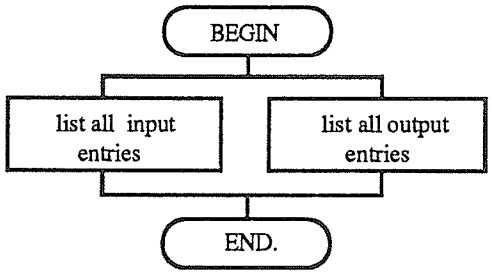

I/O

This unit is for doing all the necessary calculations and displaying all the outputs.

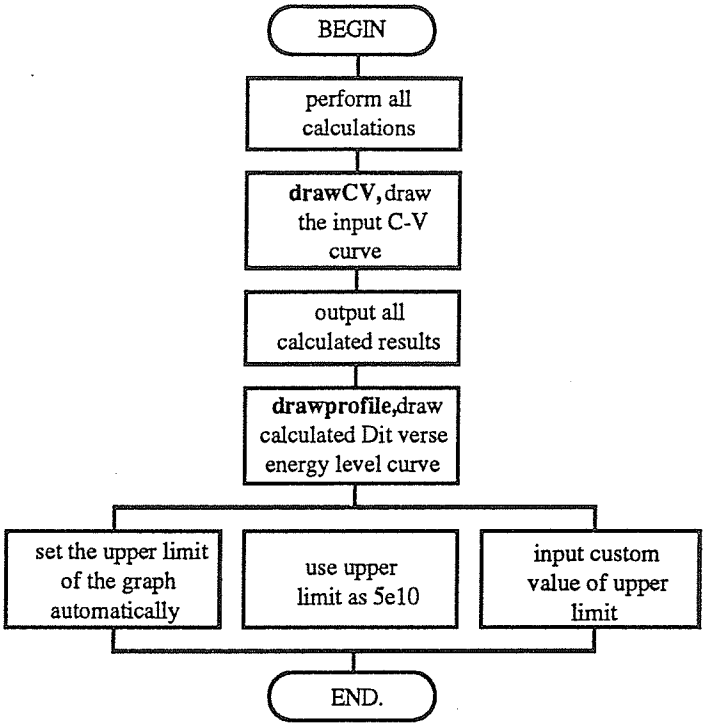

Program Listings

```
PROGRAM Dit;     {main program}

  USES
    variables, env, newdata, cdata, I_O;

  VAR
    ans : char;
    done : boolean;
    sel : boolean;
    j : integer;
    cas : integer;

BEGIN

  done := false;

  WHILE NOT done DO
    BEGIN

      hideall;
      env;

      sel := false;
      WHILE NOT sel DO
        BEGIN
          sel := true;
          writeln('[1] Input new data set');
          writeln('[2] Load data set');
          write('Input selection.   ');
          readln(cas);
          writeln;
          CASE cas OF
            1 :
              newdata;
            2 :
              BEGIN
                write('Input name of file to be load.');
                readln(filename);
                open(data, filename);
                reset(data);
                IF NOT eof(data) THEN
                  BEGIN
                    read(data, Cox, Cmin, Vgmax, Vgmin, inc);

                    max := round((Vgmax - Vgmin) / inc) + 1;

                    FOR j := 1 TO max DO
                      BEGIN
                        read(data, Clf[j], Chf[j]);
                      END;
                  END
```

```
                ELSE
                  BEGIN
                    writeln;
                    writeln('File is empty');
                    sel := false;
                  END;
                close(data);
              END;
            OTHERWISE
              sel := false;
        END;
    END;

corrected := true;
WHILE corrected DO
    BEGIN

        corrected := false;

        env;
        I_O;

    END;

sel := false;
WHILE NOT sel DO
    BEGIN

        writeln;
        writeln('[1] List Data');
        writeln('[2] Correct data');
        writeln('[3] Save Graphs ');
        writeln('[4] Continue');
        writeln('[5] Quit');

        write('Input Selection.   ');
        readln(j);
        CASE j OF
            1 :
              listdata;
            2 :
              cdata;
            3 :
              savedrawing(StringOf(filename, '.graph'));
            4 :
              BEGIN
                done := false;
                sel := true;
                writeln;
                writeln;
              END;
            5 :
              BEGIN
                done := true;
```

```
                    sel := true;
                END;
            OTHERWISE
                sel := false;
        END;
    END;

END;

END.
```

```
UNIT variables;

INTERFACE

  CONST
    pi = 3.1416;
    radius = 0.04;          {radius of capacitor in cm}
    Eg = 1.12;
    q = 1.602e-19;

  VAR
    Cox : real;
    Cmin : real;
    Vgmax : real;
    Vgmin : real;
    Vg : real;
    inc : real;
    Chf : ARRAY[1..100] OF real;
    Clf : ARRAY[1..100] OF real;
    Ene : ARRAY[1..100] OF real;
    Dit : ARRAY[1..100] OF real;

    filename : STRING[20];
    data : FILE OF real;

    t : real;               {thickness of oxide}

    corrected : boolean;
    max : integer;

IMPLEMENTATION
END.
```

```
UNIT env;

INTERFACE

  PROCEDURE drawenv;
  PROCEDURE env;

IMPLEMENTATION

  VAR

    tx : rect;
    dr : rect;
    clean : rect;

  PROCEDURE drawenv;

  BEGIN

    moveto(0, 168);
    lineto(300, 168);
    moveto(0, 171);
    lineto(300, 171);

    moveto(15, 150);
    lineto(245, 150);

    moveto(65, 320);
    lineto(245, 320);

    moveto(155, 318);
    lineto(155, 322);
    moveto(148, 332);
    writedraw('MG');
    moveto(65, 318);
    lineto(65, 322);
    moveto(63, 332);
    writedraw('Ev');
    moveto(245, 318);
    lineto(245, 322);
    moveto(243, 332);
    writedraw('Ec');

  END;


  PROCEDURE env;


  BEGIN

    setrect(tx, 0, 17, 250, 340);
    setrect(dr, 250, 0, 550, 355);
```

```
        settextrect(tx);
        setdrawingrect(dr);
        showdrawing;
        showtext;

        setrect(clean, 0, 0, 300, 355);
        eraserect(clean);

        drawenv;

    END;

END.
```

```
UNIT newdata;

INTERFACE

  USES
    variables;

  PROCEDURE newdata;

IMPLEMENTATION

  PROCEDURE newdata;

    VAR
      count : integer;
      max1 : integer;

  BEGIN

    write('Input name of data set:    ');
    readln(filename);

    open(data, filename);
    rewrite(data);

    writeln;
    write('Cox = ?[pF]    ');
    readln(Cox);
    write('Cmin = ?[pF]   ');
    readln(Cmin);

    write('Input lower limit of Vg.  ');
    readln(Vgmin);
    write('Input upper limit of Vg.  ');
    readln(Vgmax);

    write('Input step size of Vg.  ');
    readln(inc);

    max1 := round((Vgmax - Vgmin) / inc) + 1;

    Vg := Vgmin;
    writeln;
    FOR count := 1 TO max1 DO
      BEGIN
        write('Clf[', Vg : 1 : 1, '] = ');
        Clf[count] := 5;
        WHILE Clf[count] > 1 DO
          readln(Clf[count]);
        Vg := Vg + inc;
      END;

    Vg := Vgmin;
    writeln;
```

```
      FOR count := 1 TO max1 DO
        BEGIN
          write('Chf[', Vg : 1 : 1, '] = ');
          Chf[count] := 5;
          WHILE Chf[count] > 1 DO
            readln(Chf[count]);
          Vg := Vg + inc;

        END;

      write(data, Cox, Cmin, Vgmax, Vgmin, inc);

      FOR count := 1 TO max1 DO
        BEGIN
          write(data, Clf[count], Chf[count]);
        END;
      close(data);
      max := max1;
    END;

END.
```

```
UNIT cdata;

INTERFACE

  USES
    variables;

  PROCEDURE cdata;


IMPLEMENTATION

  PROCEDURE cdata;

    VAR
      j, j1 : integer;
      Vgc : real;
      Chfnew : ARRAY[1..150] OF real;
      Clfnew : ARRAY[1..150] OF real;
      Vgmax_new : real;
      Vgmin_new : real;
      ans : char;


  BEGIN

    ans := 'y';
    WHILE ans = 'y' DO
      BEGIN


          corrected := true;

          writeln;
          writeln('Select item to be change.');
          writeln('[1]:Chf  [2]:Clf  [3]:Vgmax  [4]:Vgmin');
          write('?');
          readln(j);

          CASE j OF
            1 :
              BEGIN
                write('Input at which voltage?');
                readln(Vgc);
                write('Chf[', Vgc : 1 : 2, '] = ');
                readln(Chf[round((Vgc - Vgmin) / inc) + 1]);
                Vgmax_new := Vgmax;
                Vgmin_new := Vgmin;
              END;

            2 :
              BEGIN
                write('Input at which voltage?');
                readln(Vgc);
```

```
                write('Clf[', Vgc : 1 : 2, '] = ');
                readln(Clf[round((Vgc - Vgmin) / inc) + 1]);
                Vgmax_new := Vgmax;
                Vgmin_new := Vgmin;
              END;

            3 :
              BEGIN
                write('Input new upper limit   ');
                readln(Vgmax_new);

                IF Vgmax_new > Vgmax THEN
                  BEGIN
                    Vg := Vgmax + inc;
                    FOR j1 := max + 1 TO max + round(abs(Vgmax_new - Vgmax) /
inc) DO
                      BEGIN
                        write('Clf[', Vg : 1 : 2, '] = ');
                        readln(Clf[j1]);
                        Vg := Vg + inc;
                      END;

                    Vg := Vgmax + inc;
                    FOR j1 := max + 1 TO max + round(abs(Vgmax_new - Vgmax) /
inc) DO
                      BEGIN
                        write('Chf[', Vg : 1 : 2, '] = ');
                        readln(Chf[j1]);
                        Vg := Vg + inc;
                      END;
                    max := max + round(abs(Vgmax_new - Vgmax) / inc);
                    Vgmax := Vgmax_new;

                  END
                ELSE
                  writeln('Use larger Vgmax.');

                Vgmin_new := Vgmin;
              END;

            4 :
              BEGIN
                write('Input new lower limit   ');
                readln(Vgmin_new);
                IF Vgmin_new < Vgmin THEN
                  BEGIN
                    FOR j1 := 1 TO max DO
                      BEGIN
                        Chfnew[j1] := Chf[j1];
                        Clfnew[j1] := Clf[j1];
                      END;

                    Vg := Vgmin_new;
                    FOR j1 := 1 TO round(abs(Vgmin - Vgmin_new) / inc) DO
```

```
                        BEGIN
                           write('Clf[', Vg : 1 : 2, '] = ');
                           readln(Clf[j1]);
                           Vg := Vg + inc;
                        END;

                     Vg := Vgmin_new;
                     FOR j1 := 1 TO round(abs(Vgmin - Vgmin_new) / inc) DO
                        BEGIN
                           write('Chf[', Vg : 1 : 2, '] = ');
                           readln(Chf[j1]);
                           Vg := Vg + inc;
                        END;

                     FOR j1 := 1 TO max DO
                        BEGIN
                           Chf[j1 + round(abs(Vgmin - Vgmin_new) / inc)] :=
Chfnew[j1];
                           Clf[j1 + round(abs(Vgmin - Vgmin_new) / inc)] :=
Clfnew[j1];
                        END;
                     max := max + round(abs(Vgmin - Vgmin_new) / inc);
                     Vgmin := Vgmin_new;
                  END
               ELSE
                  writeln('Use smaller lowest limit.');

               Vgmax_new := Vgmax;
            END;

         OTHERWISE
            BEGIN
               corrected := false;
               writeln('Nothing changed!');
            END;

      END;

      IF corrected THEN
         BEGIN
            open(data, filename);
            rewrite(data);
            write(data, Cox, Cmin, Vgmax_new, Vgmin_new, inc);

            FOR j := 1 TO max DO
               BEGIN
                  write(data, Clf[j], Chf[j]);
               END;
            close(data);
         END;

      writeln('[1] More corrections');
      writeln('[2] Done corrections');
      write('Input selection.    ');
```

```
            readln(j);

            j1 := 1;
            WHILE j1 = 1 DO
               BEGIN
                  j1 := 0;
                  CASE j OF
                     1 :
                        ans := 'y';
                     2 :
                        ans := 'n';
                     OTHERWISE
                        BEGIN
                           j1 := 1;
                           ans := 'y';
                        END;
                  END;
               END;
         END;
   END;
END.
```

```
UNIT I_O;

INTERFACE

  USES
    variables, newdata, cdata;

  PROCEDURE I_O;
  PROCEDURE listdata;

IMPLEMENTATION

  PROCEDURE listdata;
    VAR
      j : integer;
      sel : boolean;
      cas : integer;

  BEGIN

    writeln('[1] List input');
    writeln('[2] List output');
    write('Select input.    ');
    readln(cas);

    sel := false;
    WHILE sel = false DO
      BEGIN
        CASE cas OF
          1 :
            BEGIN
              sel := true;
              writeln;
              writeln('Cox: ', Cox : 4 : 1, '  Cmin: ', Cmin : 4 : 1);
              writeln;
              FOR j := 1 TO max DO
                BEGIN
                  write('Clf[', Vgmin + inc * (j - 1) : 1 : 2, ']:', Clf[j] : 1 : 3);
                  writeln('    Chf[', Vgmin + inc * (j - 1) : 1 : 2, ']:', Chf[j] : 1 : 3);
                END;
            END;
          2 :
            BEGIN
              sel := true;
              writeln;
              writeln;
              writeln('E[MG]-E      Dit');
              FOR j := 1 TO max DO
                BEGIN
                  writeln(ene[j], Dit[j])
                END;
            END;
          OTHERWISE
        END;
```

```
    END;
END;


PROCEDURE I_O;

  PROCEDURE drawCV;
    VAR
      Vg : real;
      count : integer;
      xinc : integer;

  BEGIN
    xinc := round(230 / ((Vgmax - Vgmin) / inc));

    moveto(15, 150 - round(Clf[1] * 100));
    count := 2;
    WHILE count <= max DO
      BEGIN
        lineto((count - 1) * xinc + 15, 150 - round(Clf[count] * 100));
        count := count + 1;
      END;

    moveto(15, 150 - round(Chf[1] * 100));
    count := 2;
    WHILE count <= max DO
      BEGIN
        lineto((count - 1) * xinc + 15, 150 - round(Chf[count] * 100));
        count := count + 1;
      END;
  END;


  PROCEDURE drawprofile;

    VAR
      E : ARRAY[1..100] OF integer;
      D : integer;
      Dmax : real;
      j : integer;
      j1 : integer;
      dummy : integer;
      dummy1 : real;
      Dmin : real;
      Emin : real;
      found : boolean;
      Ditmg : real;
      cas : integer;
      start : integer;
      smax : real;
      finish : boolean;
      re1 : rect;
```

```
BEGIN

  setrect(re1, 0, 203, 300, 320);

  FOR j := 1 TO max DO
    BEGIN
      E[j] := 155 + round(Ene[j] / 0.56 * 90);
    END;


  Dmax := 0;
  Dmin := 1e16;
  found := false;
  FOR j := 1 TO max DO
    BEGIN
      IF Dit[j] > Dmax THEN
        Dmax := Dit[j];
      IF Dit[j] < Dmin THEN
        BEGIN
          Dmin := Dit[j];
          Emin := Ene[j];
        END;

      IF ((NOT found) AND (Ene[j] >= 0)) THEN
        BEGIN
          IF Ene[j] = 0 THEN
            BEGIN
              Ditmg := Dit[j];
            END
          ELSE
            BEGIN
              IF j > 1 THEN
                BEGIN
                  found := true;
                  Ditmg := Dit[j - 1] + (Dit[j] - Dit[j - 1]) * (-Ene[j - 1] /
(Ene[j] - Ene[j - 1]));
                END
              ELSE
                BEGIN
                  found := true;
                  Ditmg := Dit[1] + (Dit[2] - Dit[1]) * (-Ene[1] / (Ene[2] -
Ene[1]));
                END;
            END;
        END;
    END;

  moveto(5, 188);
  writedraw('Dit has minimum value : ', Dmin, '  at Ev +', Emin + Eg / 2 : 1 : 2);
  moveto(5, 202);
  writedraw('Midgap Dit = ', Ditmg);

  writeln('Dit has minimum value : ', Dmin, '  at Ev +', Emin + Eg / 2 : 1 : 2);
```

```
writeln('Midgap Dit = ', Ditmg);

writeln;
finish := false;
WHILE NOT finish DO
   BEGIN
      eraserect(re1);
      moveto(62, 220);
      lineto(65, 220);
      writeln;
      writeln('[1] Autoscale');
      writeln('[2] Use maximum = 5e12');
      writeln('[3] Input maximum');
      write('Input Selection.     ');
      readln(cas);
      CASE cas OF
         1 :
            BEGIN
               moveto(13, 225);
               writedraw(Dmax);
               moveto(20, 323);
               writedraw('0');

               moveto(E[1], 320 - round(Dit[1] / Dmax * 100));
               start := 1;
               j := 2;
               WHILE (abs(Ene[j]) > (Eg / 2)) DO
                  BEGIN
                     moveto(E[j], 320 - round(Dit[j] / 5e12 * 100));
                     start := j;
                     j := j + 1;
                  END;
               FOR j := start TO max DO
                  BEGIN
                     IF (abs(Ene[j]) < (Eg / 2)) THEN
                        lineto(E[j], 320 - round(Dit[j] / Dmax * 100));
                  END;
            END;
         2 :
            BEGIN
               moveto(13, 225);
               writedraw('5e12');
               moveto(20, 323);
               writedraw('0');

               moveto(E[1], 320 - round(Dit[1] / 5e12 * 100));
               start := 2;

               j := 2;
               WHILE (Dit[j] > 5e12) OR (abs(Ene[j]) > (Eg / 2)) DO
                  BEGIN
                     moveto(E[j], 320 - round(Dit[j] / 5e12 * 100));
                     start := j;
                     j := j + 1;
```

```
                END;


                FOR j := start TO max DO
                  BEGIN
                    IF (Dit[j] <= 5e12) AND (abs(Ene[j]) < (Eg / 2)) THEN
                      lineto(E[j], 320 - round(Dit[j] / 5e12 * 100));
                  END;
              END;
            3 :
              BEGIN
                write('Input maximum scale.  [e10]');
                readln(smax);

                moveto(13, 225);
                writedraw(smax : 3 : 1, 'e+10');
                moveto(20, 323);
                writedraw('0');
                smax := smax * 1e10;

                moveto(E[1], 320 - round(Dit[1] / smax * 100));
                start := 2;
                j := 2;
                WHILE (Dit[j] > smax) OR (abs(Ene[j]) > (Eg / 2)) DO
                  BEGIN
                    moveto(E[j], 320 - round(Dit[j] / smax * 100));
                    start := j;
                    j := j + 1;
                  END;

                FOR j := start TO max DO
                  BEGIN
                    IF (Dit[j] <= smax) AND (abs(Ene[j]) < (Eg / 2)) THEN
                      lineto(E[j], 320 - round(Dit[j] / smax * 100));
                  END;
              END;
            OTHERWISE
          END;
          writeln;
          writeln('[1] Rescale');
          writeln('[2] Done');
          write('Input Selection.    ');
          readln(j);
          IF j = 2 THEN
            finish := true;
        END;

END;

VAR
  num_inc : integer;
  area : real;
  C, Cx, Cn : real;
  k, i, l : real;
```

```
    n : real;
    Vb, Cs, Cf, Vms : real;
    count : integer;
    si : real;
    j : integer;
    FBnum : integer;
    ans : char;
    zero : integer;
    FB : integer;
    found : boolean;

BEGIN

  writeln;
  writeln('Cox: ', Cox : 4 : 1, '  Cmin: ', Cmin : 4 : 1);
  writeln;

  zero := round(abs(Vgmin / (Vgmax + abs(Vgmin)) * 230)) + 15;
  moveto(zero, 40);
  lineto(zero, 152);
  moveto(zero - 2, 162);
  writedraw('0');

  moveto(zero - 2, 50);
  lineto(zero + 2, 50);
  moveto(zero - 20, 50);
  writedraw('Cox');

  writeln;
  area := pi * radius * radius;
  t := 3.9 * 0.08854 * area / Cox * 1e8;
  writeln('Assuming gate radius is 0.04 cm');
  writeln('Oxide thickness is   ', t : 6 : 1, '  ang');
  moveto(5, 29);
  writedraw(filename, '    Oxide thickness is   ', t : 6 : 1, '  ang');
  writeln;
  writeln;
  Cx := 3.9 * 8.854e-6 / t;
  Cn := Cmin / area * 1e-12;
  C := 0.00016 * sqr(106.25e-14 / Cn - t * 3.077e-8) / 1.105e-13;

  moveto(13, 162);
  writedraw(Vgmin : 1 : 2);
  moveto(240, 162);
  writedraw(Vgmax : 1 : 2);

  i := 1;
  k := ln(i);
  l := C * i - 11.1;
  WHILE abs(k - l) > 0.1 DO
    BEGIN
      IF k - l > 0.05 THEN
        i := i + 0.01;
      IF k - l < -0.05 THEN
```

```
            i := i - 0.01;
          k := ln(i);
          l := C * i - 11.1;

        END;
      n := i * 1e15;

      writeln;
      writeln('Dopant concentration : ', n);


      Vb := 0.026 * ln(n / 1.5e10);
      Cs := sqrt(12 * 8.854e-14 * 1.6e-19 * n / 0.026);
      Cf := cs / (cs + cx);
      Vms := Vb - 0.6;
      writeln('Cfb/Cox=  ', Cf : 2 : 2, ';    Vms =  ', Vms : 2 : 2);
      moveto(5, 38);
      writedraw('   Cfb/Cox=', Cf : 1 : 2, '; Vms =', Vms : 2 : 2);


      drawCV;

{**************  E-Ec  ********************}

      IF Chf[max] > Chf[1] THEN
        BEGIN
          writeln('Substrate is N type.');
          j := 0;
          found := false;
          WHILE NOT found DO
            BEGIN
              j := j + 1;
              IF Chf[j] >= Cf THEN
                BEGIN
                  found := true;
                  FBnum := j;
                END;
            END;
        END
      ELSE
        BEGIN
          writeln('Substrate is P type.');
          j := 0;
          found := false;
          WHILE NOT found DO
            BEGIN
              j := j + 1;
              IF Chf[j] <= Cf THEN
                BEGIN
                  found := true;
                  FBnum := j;
                END;
            END;
        END;
```

```
        IF abs(Chf[FBnum] - Cf) > abs(Chf[FBnum - 1] - Cf) THEN
           FBnum := FBnum - 1;
        writeln;

        Vg := Vgmin;
        count := 1;
        WHILE count <= max DO
           BEGIN

              IF count <= FBnum THEN
                 BEGIN
                    si := -inc / 2 * ((1 - Clf[count]) + (1 - Clf[FBnum]));
                    FOR j := count + 1 TO (FBnum - 1) DO
                       BEGIN
                          si := si - inc * (1 - Clf[j]);
                       END;
                 END

              ELSE
                 BEGIN
                    si := inc / 2 * ((1 - Clf[FBnum]) + (1 - Clf[count]));
                    FOR j := (FBnum + 1) TO count - 1 DO
                       BEGIN
                          si := si + inc * (1 - Clf[j]);
                       END;
                 END;

              Ene[count] := (Eg / 2) + si - Vb;

              Dit[count] := Cox * 1e-12 / area / q;
              Dit[count] := Dit[count] * (Clf[count] / (1 - Clf[count]) - Chf[count] / (1 -
Chf[count]));

              count := count + 1;
              Vg := Vg + inc;

           END;
        drawprofile;

     END;
END.
```